
TRS: Transferability Reduced Ensemble via Promoting Gradient Diversity and Model Smoothness

Zhuolin Yang^{1*} Linyi Li^{1*} Xiaojun Xu^{1*} Shiliang Zuo¹
 Qian Chen² Benjamin Rubinstein³ Pan Zhou⁴ Ce Zhang⁵ Bo Li¹

¹ University of Illinois Urbana-Champaign ² Tencent Inc. ³ University of Melbourne

⁴ Huazhong University of Science and Technology ⁵ ETH Zurich
 {zhuolin5, linyi2, xiaojun3, szuo3, lbo}@illinois.edu
 qianchen@tencent.com
 benjamin.rubinstein@unimelb.edu.au
 panzhou@hust.edu.cn
 ce.zhang@inf.ethz.ch

Abstract

Adversarial Transferability is an intriguing property – adversarial perturbation crafted against one model is also effective against another model, while these models are from different model families or training processes. To better protect ML systems against adversarial attacks, several questions are raised: *what are the sufficient conditions for adversarial transferability and how to bound it? Is there a way to reduce the adversarial transferability in order to improve the robustness of an ensemble ML model?* To answer these questions, in this work we first theoretically analyze and outline sufficient conditions for adversarial transferability between models; then propose a practical algorithm to reduce the transferability between base models within an ensemble to improve its robustness. Our theoretical analysis shows that only promoting the orthogonality between gradients of base models is not enough to ensure low transferability; in the meantime, the model smoothness is an important factor to control the transferability. We also provide the lower and upper bounds of adversarial transferability under certain conditions. Inspired by our theoretical analysis, we propose an effective **Transferability Reduced Smooth (TRS)** ensemble training strategy to train a robust ensemble with low transferability by enforcing both gradient orthogonality and model smoothness between base models. We conduct extensive experiments on TRS and compare with 6 state-of-the-art ensemble baselines against 8 whitebox attacks on different datasets, demonstrating that the proposed TRS outperforms all baselines significantly.

1 Introduction

Machine learning systems, especially those based on deep neural networks (DNNs), have been widely applied in numerous applications [27, 18, 46, 10]. However, recent studies show that DNNs are vulnerable to adversarial examples, which are able to mislead DNNs by adding small magnitude of perturbations to the original instances [47, 17, 54, 52]. Several attack strategies have been proposed so far to generate such adversarial examples in both digital and physical environments [36, 32, 51, 53, 15, 28]. Intriguingly, though most attacks require access to the target models (whitebox attacks), several studies show that adversarial examples generated against one model are able to *transferably*

*The authors contributed equally.

attack another target model with high probability, giving rise to blackbox attacks [39, 41, 31, 30, 57]. This property of *adversarial transferability* poses great threat to DNNs.

Some work have been conducted to understand *adversarial transferability* [48, 33, 12]. However, a rigorous theoretical analysis or explanation for transferability is still lacking in the literature. In addition, although developing robust ensemble models to limit transferability shows great potential towards practical robust learning systems, only *empirical* observations have been made in this line of research [38, 23, 56]. *Can we deepen our theoretical understanding on transferability? Can we take advantage of rigorous theoretical understanding to reduce the adversarial transferability and therefore generate robust ensemble ML models?*

In this paper, we focus on these two questions. From the theoretical side, we are interested in the sufficient conditions under which the adversarial transferability can be *lower bounded* and *upper bounded*. Our theoretical arguments provides the *first* theoretical interpretation for the sufficient conditions of transferability. Intuitively, as illustrated in Figure 1, we show that the commonly used gradient orthogonality (low cosine similarity) between learning models [12] cannot directly imply low adversarial transferability; on the other hand, orthogonal and smoothed models would limit the transferability. In particular, we prove that the *gradient similarity* and *model smoothness* are the key factors that both contribute to the adversarial transferability, and smooth models with orthogonal gradients can guarantee low transferability.

Under an empirical lens, inspired by our theoretical analysis, we propose a simple yet effective approach, **Transferability Reduced Smooth (TRS)** ensemble to limit adversarial transferability between base models within an ensemble and therefore improve its robustness. In particular, we reduce the loss gradient similarity between models as well as enforce the smoothness of models to introduce global model orthogonality.

We conduct extensive experiments to evaluate TRS in terms of the model robustness against different strong white-box and blackbox attacks following the robustness evaluation procedures [5, 6, 49], as well as its ability to limit transferability across the base models. We compare the proposed TRS with existing state-of-the-art baseline ensemble approaches such as ADP [38], GAL [23], and DVERGE [56] on MNIST, CIFAR-10, and CIFAR-100 datasets, and we show that (1) TRS achieves the state-of-the-art ensemble robustness, outperforming others by a large margin; (2) TRS achieves efficient training; (3) TRS effectively reduces the transferability among base models within an ensemble which indicates its robustness against whitebox and blackbox attacks; (4) Both loss terms in TRS contribute to the ensemble robustness by constraining different sufficient conditions of adversarial transferability.

Contributions. In this paper, we make the first attempt towards theoretical understanding of adversarial transferability, and provide practical approach for developing robust ML ensembles.

- (1) We provide a general theoretical analysis framework for adversarial transferability. We prove the lower and upper bounds of adversarial transferability. Both bounds show that the gradient similarity and model smoothness are the key factors contributing to the adversarial transferability, and smooth models with orthogonal gradients can guarantee low transferability.
- (2) We propose a simple yet effective approach TRS to train a robust ensemble by jointly reducing the loss gradient similarity between base models and enforcing the model smoothness. The code is publicly available².
- (3) We conduct extensive experiments to evaluate TRS in terms of model robustness under different attack settings, showing that TRS achieves the state-of-the-art ensemble robustness and outperforms other baselines by a large margin. We also conduct ablation studies to further understand the contribution of different loss terms and verify our theoretical findings.

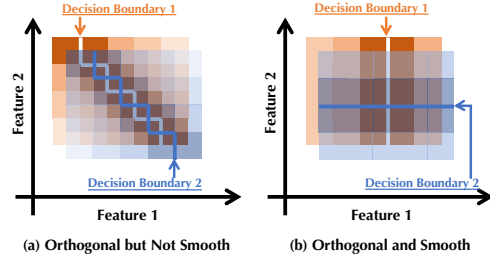


Figure 1: An illustration of the relationship between *adversarial transferability*, *gradient orthogonality*, and *model smoothness*. (a) Gradient orthogonality alone cannot minimize transferability as the decision boundaries between two classifiers can be arbitrarily close yet orthogonal almost everywhere; (b) Gradient orthogonality with model smoothness provides a stronger guarantee on model diversity, as our theorems will show.

²<https://github.com/AI-secure/Transferability-Reduced-Smooth-Ensemble>

Related Work

The adversarial transferability between different ML models is an intriguing research direction. Papernot et al. [40] explored the limitation of adversarial examples and showed that, while some instances are more difficult to manipulate than the others, these adversarial examples usually transfer from one model to another. Demontis et al. [12] later analyzed transferability for both evasion and poisoning attacks. Tramèr et al. [48] empirically investigated the subspace of adversarial examples that enables transferability between different models: though their results provide a non-zero probability guarantee on the transferability, they did not quantify the probability of adversarial transferability.

Leveraging the transferability, different blackbox attacks have been proposed [41, 28, 15, 9]. To defend against these transferability based attacks, Pang et al. [38] proposed a class entropy based adaptive diversity promoting approach to enhance the ML ensemble robustness. Recently, Yang et al. [56] proposed DVERGE, a robust ensemble training approach that diversifies the non-robust features of base models via an adversarial training objective function. However, these approaches do not provide theoretical justification for adversarial transferability, and there is still room to improve the ML ensemble robustness based on in-depth understanding on the sufficient conditions of transferability. In this paper, we aim to provide a theoretical understanding of transferability, and empirically compare the proposed robust ML ensemble inspired by our theoretical analysis with existing approaches to push for a tighter empirical upper bound for the ensemble robustness.

2 Transferability of Adversarial Perturbation

In this section, we first introduce preliminaries, and then provide the upper and lower bounds of adversarial transferability by connecting adversarial transferability with different characteristics of models theoretically, which, in the next section, will allow us to explicitly minimize transferability by enforcing (or rewarding) certain properties of models.

Notations. We consider neural networks for classification tasks. Assume there are C classes, and let \mathcal{X} be the *input space* of the model with $\mathcal{Y} = \{1, 2, \dots, C\}$ the set of prediction classes (i.e., labels). We model the neural network by a mapping function $\mathcal{F} : \mathcal{X} \rightarrow \mathcal{Y}$. We will study the transferability between two models \mathcal{F} and \mathcal{G} . For brevity, hereinafter we mainly show the derived notations for \mathcal{F} and notations for \mathcal{G} are similar. Let the *benign* data (x, y) follow an unknown distribution \mathcal{D} supported on $(\mathcal{X}, \mathcal{Y})$, and $\mathcal{P}_{\mathcal{X}}$ denote the marginal distribution on \mathcal{X} .

For a given input $x \in \mathcal{X}$, the classification model \mathcal{F} first predicts the confidence score for each label $y \in \mathcal{Y}$, denoted as $f_y(x)$. These confidence scores sum up to 1, i.e., $\sum_{y \in \mathcal{Y}} f_y(x) = 1, \forall x \in \mathcal{X}$. The model \mathcal{F} will predict the label with highest confidence score: $\mathcal{F}(x) = \arg \max_{y \in \mathcal{Y}} f_y(x)$.

For model \mathcal{F} , there is usually a model-dependent loss function $\ell_{\mathcal{F}} : \mathcal{X} \times \mathcal{Y} \rightarrow \mathbb{R}_+$, which is the composition of a differentiable training loss (e.g., cross-entropy loss) ℓ and the model’s confidence score $f(\cdot)$: $\ell_{\mathcal{F}}(x, y) := \ell(f(x), y), (x, y) \in (\mathcal{X}, \mathcal{Y})$. We further assume that $\mathcal{F}(x) = \arg \min_{y \in \mathcal{Y}} \ell_{\mathcal{F}}(x, y)$, i.e., the model predicts the label with minimum loss. This holds for common training losses.

In this paper, by default we will focus on models that are well-trained on the benign dataset, and such models are the most commonly encountered in practice, so their robustness is paramount. This means we will focus on the *low risk* classifiers, which we will formally define in Section 2.1.

How should we define an adversarial attack? For the threat model, we consider the attacker that adds an ℓ_p norm bounded perturbation to data instance $x \in \mathcal{X}$. In practice, there are two types of attacks, *untargeted attacks* and *targeted attacks*. The definition of adversarial transferability is slightly different under these attacks [33], and we consider both in our analysis.

Definition 1 (Adversarial Attack). *Given an input $x \in \mathcal{X}$ with true label $y \in \mathcal{Y}$, $\mathcal{F}(x) = y$. (1) An untargeted attack crafts $\mathcal{A}_U(x) = x + \delta$ to maximize $\ell_{\mathcal{F}}(x + \delta, y)$ where $\|\delta\|_p \leq \epsilon$. (2) A targeted attack with target label $y_t \in \mathcal{Y}$ crafts $\mathcal{A}_T(x) = x + \delta$ to minimize $\ell_{\mathcal{F}}(x + \delta, y_t)$ where $\|\delta\|_p \leq \epsilon$.*

In this definition, ϵ is a pre-defined *attack radius* that limits the power of the attacker. We may refer to $\{\delta : \|\delta\|_p \leq \epsilon\}$ as the perturbation ball. The goal of the untargeted attack is to maximize the loss of the target model against its true label y . The goal of the targeted attack is to minimize the loss towards its adversarial target label y_t .

How do we formally define that an attack is effective?

Definition 2 ((α, \mathcal{F}) -Effective Attack). Consider a input $x \in \mathcal{X}$ with true label $y \in \mathcal{Y}$. An attack is (α, \mathcal{F}) -effective in untargeted scenario if $\Pr(\mathcal{F}(\mathcal{A}_U(x)) \neq y) \geq 1 - \alpha$. An attack is (α, \mathcal{F}) -effective in targeted scenario (with class target y_t) if $\Pr(\mathcal{F}(\mathcal{A}_T(x)) = y_t) \geq 1 - \alpha$.

This definition captures the requirement that an adversarial instance generated by an effective attack strategy is able to mislead the target classification model (e.g. \mathcal{F}) with certain probability $(1 - \alpha)$. The smaller the α is, the more effective the attack is. In practice, this implies that on a finite sample of targets, the attack success is frequent but not absolute. Note that the definition is general for both whitebox [1, 12, 5] and blackbox attacks [42, 4].

2.1 Model Characteristics

Given two models \mathcal{F} and \mathcal{G} , what are the characteristics of \mathcal{F} and \mathcal{G} that have impact on transferability under a given attack strategy? Intuitively, the more similar these two classifiers are, the larger the transferability would be. However, how can we define “similar” and how can we rigorously connect it to transferability? To answer these questions, we will first define the risk and empirical risk for a given model to measure its performance on benign test data. Then, as the DNNs are differentiable, we will define model similarity based on their gradients. We will then derive the lower and upper bounds of adversarial transferability based on the defined model risk and similarity measures.

Definition 3 (Risk and Empirical Risk). For a given model \mathcal{F} , we let $\ell_{\mathcal{F}}$ be its model-dependent loss function. Its **risk** is defined as $\eta_{\mathcal{F}} = \Pr(\mathcal{F}(x) \neq y)$; and its **empirical risk** is defined as $\xi_{\mathcal{F}} = \mathbb{E}[\ell_{\mathcal{F}}(x, y)]$.

The *risk* represents the model’s error rate on benign test data, while the *empirical risk* is a non-negative value that also indicates the inaccuracy. For both of them, higher value means worse performance on the benign test data. The difference is that, the risk has more intuitive meaning, while the empirical risk is differentiable and is actually used during model training.

Definition 4 (Loss Gradient Similarity). The lower loss gradient similarity $\underline{\mathcal{S}}$ and upper loss gradient similarity $\overline{\mathcal{S}}$ between two differentiable loss functions $\ell_{\mathcal{F}}$ and $\ell_{\mathcal{G}}$ is defined as:

$$\underline{\mathcal{S}}(\ell_{\mathcal{F}}, \ell_{\mathcal{G}}) = \inf_{x \in \mathcal{X}, y \in \mathcal{Y}} \frac{\nabla_x \ell_{\mathcal{F}}(x, y) \cdot \nabla_x \ell_{\mathcal{G}}(x, y)}{\|\nabla_x \ell_{\mathcal{F}}(x, y)\|_2 \cdot \|\nabla_x \ell_{\mathcal{G}}(x, y)\|_2}, \overline{\mathcal{S}}(\ell_{\mathcal{F}}, \ell_{\mathcal{G}}) = \sup_{x \in \mathcal{X}, y \in \mathcal{Y}} \frac{\nabla_x \ell_{\mathcal{F}}(x, y) \cdot \nabla_x \ell_{\mathcal{G}}(x, y)}{\|\nabla_x \ell_{\mathcal{F}}(x, y)\|_2 \cdot \|\nabla_x \ell_{\mathcal{G}}(x, y)\|_2}.$$

The $\underline{\mathcal{S}}(\ell_{\mathcal{F}}, \ell_{\mathcal{G}})$ ($\overline{\mathcal{S}}(\ell_{\mathcal{F}}, \ell_{\mathcal{G}})$) is the minimum (maximum) cosine similarity between the gradients of the two loss functions for an input x drawn from \mathcal{X} with any label $y \in \mathcal{Y}$. Besides the loss gradient similarity, in our analysis we will also show that the *model smoothness* is another key characteristic of ML models that affects the model transferability.

Definition 5. We call a model \mathcal{F} β -smooth if $\sup_{x_1, x_2 \in \mathcal{X}, y \in \mathcal{Y}} \frac{\|\nabla_x \ell_{\mathcal{F}}(x_1, y) - \nabla_x \ell_{\mathcal{F}}(x_2, y)\|_2}{\|x_1 - x_2\|_2} \leq \beta$.

This smoothness definition is commonly used in deep learning theory and optimization literature [3, 2], and is also named curvature bounds in certified robustness literature [44]. It could be interpreted as the Lipschitz bound for the model’s loss function gradient. We remark that *larger* β indicates that the model is less smoother, while *smaller* β means the model is smoother. Particularly, when $\beta = 0$, the model is linear in the input space \mathcal{X} .

2.2 Definition of Adversarial Transferability

Based on the model characteristics we explored above, next we will ask: *Given two models, what is the natural and precise definition of adversarial transferability?*

Definition 6 (Transferability). Consider an adversarial instance $\mathcal{A}_U(x)$ or $\mathcal{A}_T(x)$ constructed against a surrogate model \mathcal{F} . With a given benign input $x \in \mathcal{X}$, The transferability T_r between \mathcal{F} and a target model \mathcal{G} is defined as follows (adversarial target $y_t \in \mathcal{Y}$):

- *Untargeted:* $T_r(\mathcal{F}, \mathcal{G}, x) = \mathbb{I}[\mathcal{F}(x) = \mathcal{G}(x) = y \wedge \mathcal{F}(\mathcal{A}_U(x)) \neq y \wedge \mathcal{G}(\mathcal{A}_U(x)) \neq y]$.
- *Targeted:* $T_r(\mathcal{F}, \mathcal{G}, x, y_t) = \mathbb{I}[\mathcal{F}(x) = \mathcal{G}(x) = y \wedge \mathcal{F}(\mathcal{A}_T(x)) = \mathcal{G}(\mathcal{A}_T(x)) = y_t]$.

Here we define the transferability at instance level, showing several conditions are required to satisfy for a transferable instance. For the untargeted attack, it requires that: (1) both the surrogate model

and target model make correct prediction on the benign input; and (2) both of them make incorrect predictions on the adversarial input $\mathcal{A}_U(x)$. The $\mathcal{A}_U(x)$ is generated via the untargeted attack against the surrogate model \mathcal{F} . For the targeted attack, it requires that: (1) both the surrogate and target model make correct prediction on benign input; and (2) both output the adversarial target $y_t \in \mathcal{Y}$ on the adversarial input $\mathcal{A}_T(x)$. The $\mathcal{A}_T(x)$ is crafted against the surrogate model \mathcal{F} . The predicates themselves do not require \mathcal{A}_U and \mathcal{A}_T to be explicitly constructed against the surrogate model \mathcal{F} . It will be implied by attack effectiveness (Definition 2) on \mathcal{F} in theorem statements. Note that the definition here is a predicate for a specific input x , and in the following analysis we will mainly use its distributional version: $\Pr(T_r(\mathcal{F}, \mathcal{G}, x) = 1)$ and $\Pr(T_r(\mathcal{F}, \mathcal{G}, x, y_t) = 1)$.

2.3 Lower Bound of Adversarial Transferability

Based on the general definition of transferability, in this section we will analyze how to lower bound the transferability for targeted attack. The analysis for untargeted attack has a similar form and is deferred to Theorem 3 in Appendix A.

Theorem 1 (Lower Bound on Targeted Attack Transferability). *Assume both models \mathcal{F} and \mathcal{G} are β -smooth. Let \mathcal{A}_T be an (α, \mathcal{F}) -effective targeted attack with perturbation ball $\|\delta\|_2 \leq \epsilon$ and target label $y_t \in \mathcal{Y}$. The transferability can be lower bounded by*

$$\Pr(T_r(\mathcal{F}, \mathcal{G}, x, y_t) = 1) \geq (1-\alpha) - (\eta_{\mathcal{F}} + \eta_{\mathcal{G}}) - \frac{\epsilon(1+\alpha) + c_{\mathcal{F}}(1-\alpha)}{c_{\mathcal{G}} + \epsilon} - \frac{\epsilon(1-\alpha)}{c_{\mathcal{G}} + \epsilon} \sqrt{2 - 2\underline{\mathcal{S}}(\ell_{\mathcal{F}}, \ell_{\mathcal{G}})},$$

where

$$c_{\mathcal{F}} = \max_{x \in \mathcal{X}} \frac{\min_{y \in \mathcal{Y}} \ell_{\mathcal{F}}(\mathcal{A}_T(x), y) - \ell_{\mathcal{F}}(x, y_t) + \beta\epsilon^2/2}{\|\nabla_x \ell_{\mathcal{F}}(x, y_t)\|_2}, \quad c_{\mathcal{G}} = \min_{x \in \mathcal{X}} \frac{\min_{y \in \mathcal{Y}} \ell_{\mathcal{G}}(\mathcal{A}_T(x), y) - \ell_{\mathcal{G}}(x, y_t) - \beta\epsilon^2/2}{\|\nabla_x \ell_{\mathcal{G}}(x, y_t)\|_2}.$$

Here $\eta_{\mathcal{F}}, \eta_{\mathcal{G}}$ are the risks of models \mathcal{F} and \mathcal{G} respectively.

We defer the complete proof in Appendix C. In the proof, we first use a Taylor expansion to introduce the gradient terms, then relate the dot product with cosine similarity of the loss gradients, and finally use Markov's inequality to derive the misclassification probability of \mathcal{G} to complete the proof.

Implications. In Theorem 1, the only term which correlates both \mathcal{F} and \mathcal{G} is $\underline{\mathcal{S}}(\ell_{\mathcal{F}}, \ell_{\mathcal{G}})$, while all other terms depend on individual models \mathcal{F} or \mathcal{G} . Thus, we study the relation between $\underline{\mathcal{S}}(\ell_{\mathcal{F}}, \ell_{\mathcal{G}})$ and $\Pr(T_r(\mathcal{F}, \mathcal{G}, x, y_t) = 1)$.

Note that since β is small compared with the perturbation radius ϵ and the gradient magnitude $\|\nabla_x \ell_{\mathcal{G}}\|_2$ in the denominator is relatively large, the quantity $c_{\mathcal{G}}$ is small. Moreover, $1 - \alpha$ is large since the attack is typically effective against \mathcal{F} . Thus, $\Pr(T_r(\mathcal{F}, \mathcal{G}, x, y_t) = 1)$ has the form $C - k\sqrt{1 - \underline{\mathcal{S}}(\ell_{\mathcal{F}}, \ell_{\mathcal{G}})}$, where C and k are both positive constants. We can easily observe the *positive* correlation between the loss gradients similarity $\underline{\mathcal{S}}(\ell_{\mathcal{F}}, \ell_{\mathcal{G}})$, and lower bound of adversarial transferability $\Pr(T_r(\mathcal{F}, \mathcal{G}, x, y_t) = 1)$.

In the meantime, note that when β increases (i.e., model becomes less smooth), in the transferability lower bound $C - k\sqrt{1 - \underline{\mathcal{S}}(\ell_{\mathcal{F}}, \ell_{\mathcal{G}})}$, the C decreases and k increase. As a result, the lower bounds in Theorem 1 decreases, which implies that when model becomes less smoother (i.e., β becomes larger), the transferability lower bounds become looser for both targeted and untargeted attacks. In other words, *when the model becomes smoother, the correlation between loss gradients similarity and lower bound of transferability becomes stronger*, which motivates us to constrain the model smoothness to increase the effect of limiting loss gradients similarity.

In addition to the ℓ_p -bounded attacks, we also derive a transferability lower bound for general attacks whose magnitude is bounded by total variance distance of data distributions. We defer the detail analysis and discussion to Appendix B.

2.4 Upper Bound of Adversarial Transferability

We next aim to upper bound the adversarial transferability. The upper bound for target attack is shown below; and the one for untargeted attack has a similar form in Theorem 4 in Appendix A.

Theorem 2 (Upper Bound on Targeted Attack Transferability). *Assume both models \mathcal{F} and \mathcal{G} are β -smooth with gradient magnitude bounded by B , i.e., $\|\nabla_x \ell_{\mathcal{F}}(x, y)\| \leq B$ and $\|\nabla_x \ell_{\mathcal{G}}(x, y)\| \leq B$ for any $x \in \mathcal{X}, y \in \mathcal{Y}$. Let \mathcal{A}_T be an (α, \mathcal{F}) -effective targeted attack with perturbation ball $\|\delta\|_2 \leq \epsilon$*

and target label $y_t \in \mathcal{Y}$. When the attack radius ϵ is small such that $\ell_{\min} - \epsilon B \left(1 + \sqrt{\frac{1 + \bar{S}(\ell_{\mathcal{F}}, \ell_{\mathcal{G}})}{2}}\right) - \beta \epsilon^2 > 0$, the transferability can be upper bounded by

$$\Pr(T_r(\mathcal{F}, \mathcal{G}, x, y_t) = 1) \leq \frac{\xi_{\mathcal{F}} + \xi_{\mathcal{G}}}{\ell_{\min} - \epsilon B \left(1 + \sqrt{\frac{1 + \bar{S}(\ell_{\mathcal{F}}, \ell_{\mathcal{G}})}{2}}\right) - \beta \epsilon^2},$$

where $\ell_{\min} = \min_{x \in \mathcal{X}} (\ell_{\mathcal{F}}(x, y_t), \ell_{\mathcal{G}}(x, y_t))$. Here $\xi_{\mathcal{F}}$ and $\xi_{\mathcal{G}}$ are the empirical risks of models \mathcal{F} and \mathcal{G} respectively, defined relative to a differentiable loss.

We defer the complete proof to Appendix D. In the proof, we first take a Taylor expansion on the loss function at (x, y) , then use the fact that the attack direction will be dissimilar with at least one of the model gradients to upper bound the transferability probability.

Implications. In Theorem 2, we observe that along with the increase of $\bar{S}(\ell_{\mathcal{F}}, \ell_{\mathcal{G}})$, the denominator decreases and henceforth the upper bound increases. Therefore, $\bar{S}(\ell_{\mathcal{F}}, \ell_{\mathcal{G}})$ —upper loss gradient similarity and the upper bound of transferability probability is positively correlated. This tendency is the same as that in the lower bound. Note that α does not appear in upper bounds since only completely successful attacks ($\alpha = 0\%$) needs to be considered here to upper bound the transferability.

Meanwhile, when the model becomes smoother (i.e., β decreases), the transferability upper bound decreases and becomes tighter. This implication again motivates us to constrain the model smoothness. We further observe that smaller magnitude of gradient, i.e., B , also helps to tighten the upper bound. We will regularize both B and β to increase the effect of constraining loss gradients similarity.

Note that the lower bound and upper bound jointly show smaller β leads to a reduced gap between lower and upper bounds and thus a stronger correlation between loss gradients similarity and transferability. Therefore, it is important to *both* constrain gradient similarity and increase model smoothness (decrease β) to reduce model transferability and improve ensemble robustness.

3 Improving Ensemble Robustness via Transferability Minimization

Motivated by our theoretical analysis, we propose a lightweight yet effective robust ensemble training approach, **Transferability Reduced Smooth (TRS)**, to reduce the transferability among base models by enforcing *low loss gradient similarity* and *model smoothness* at the same time.

3.1 TRS Regularizer

In practice, it is challenging to directly regularize the model smoothness. Luckily, inspired from deep learning theory and optimization [14, 37, 45], succinct ℓ_2 regularization on the gradient terms $\|\nabla_x \ell_{\mathcal{F}}\|_2$ and $\|\nabla_x \ell_{\mathcal{G}}\|_2$ can reduce the magnitude of gradients and thus improve **model smoothness**. For example, for common neural networks, the smoothness can be upper bounded via bounding the ℓ_2 magnitude of gradients [45, Corollary 4]. An intuitive explanation is that, the ℓ_2 regularization on the gradient terms reduces the magnitude of model’s weights, thus limits its changing rate when non-linear activation functions are applied to the neural network model. However, we find that directly regularizing the loss gradient magnitude with ℓ_2 norm is not enough, since a vanilla ℓ_2 regularizer such as $\|\nabla_x \ell_{\mathcal{F}}\|_2$ will only focus on the local region at data point x , while it is required to ensure the model smoothness over a large decision region to control the adversarial transferability based on our theoretical analysis.

To address this challenge, we propose a min-max framework to regularize the “support” instance \hat{x} with “worst” smoothness in the neighborhood region of data point x , which results in the following model smoothness loss:

$$\mathcal{L}_{\text{smooth}}(\mathcal{F}, \mathcal{G}, x, \delta) = \max_{\|\hat{x} - x\|_{\infty} \leq \delta} \|\nabla_{\hat{x}} \ell_{\mathcal{F}}\|_2 + \|\nabla_{\hat{x}} \ell_{\mathcal{G}}\|_2 \quad (1)$$

where δ refers to the radius of the ℓ_{∞} ball around instance x within which we aim to ensure the model to be smooth. In practice, we leverage projection gradient descent optimization to search for support instances \hat{x} for optimization. This model smoothness loss can be viewed as promoting margin-wise smoothness, i.e., improving the margin between nonsmooth decision boundaries and data point x . Another option is to promote point-wise smoothness that only requires the loss landscape

at data point x itself to be smooth. We compare the ensemble robustness of the proposed min-max framework which promotes the margin-wise smoothness with the naïve baseline which directly applies ℓ_2 regularization on each model loss gradient terms to promote the point-wise smoothness (i.e. Cos- ℓ_2) in Section 4.

Given trained “smoothed” base models, we also decrease the model **loss gradient similarity** to reduce the overall adversarial transferability between base models. Among various metrics which measure the similarity between the loss gradients of base model \mathcal{F} and \mathcal{G} , we find that the vanilla cosine similarity metric, which is also used in [23], may lead to certain concerns. By minimizing the cosine similarity between $\nabla_x \ell_{\mathcal{F}}$ and $\nabla_x \ell_{\mathcal{G}}$, the optimal case implies $\nabla_x \ell_{\mathcal{F}} = -\nabla_x \ell_{\mathcal{G}}$, which means two models have contradictory (rather than diverse) performance on instance x and thus results in turbulent model functionality. Considering this challenge, we leverage the absolute value of cosine similarity between $\nabla_x \ell_{\mathcal{F}}$ and $\nabla_x \ell_{\mathcal{G}}$ as *similarity loss* \mathcal{L}_{sim} and its optimal case implies orthogonal loss gradient vectors. For simplification, we will always use the absolute value of the gradient cosine similarity as the indicator of *gradient similarity* in our later description and evaluation.

Based on our theoretical analysis and particularly the model *loss gradient similarity* and *model smoothness* optimization above, we propose TRS regularizer for model pair $(\mathcal{F}, \mathcal{G})$ on input x as:

$$\begin{aligned} \mathcal{L}_{\text{TRS}}(\mathcal{F}, \mathcal{G}, x, \delta) &= \lambda_a \cdot \mathcal{L}_{\text{sim}} + \lambda_b \cdot \mathcal{L}_{\text{smooth}} \\ &= \lambda_a \cdot \left| \frac{(\nabla_x \ell_{\mathcal{F}})^\top (\nabla_x \ell_{\mathcal{G}})}{\|\nabla_x \ell_{\mathcal{F}}\|_2 \cdot \|\nabla_x \ell_{\mathcal{G}}\|_2} \right| + \lambda_b \cdot \left[\max_{\|\hat{x}-x\|_\infty \leq \delta} \|\nabla_{\hat{x}} \ell_{\mathcal{F}}\|_2 + \|\nabla_{\hat{x}} \ell_{\mathcal{G}}\|_2 \right]. \end{aligned}$$

Here $\nabla_x \ell_{\mathcal{F}}$ and $\nabla_x \ell_{\mathcal{G}}$ refer to the loss gradient vectors of base models \mathcal{F} and \mathcal{G} on input x , and λ_a, λ_b the weight balancing parameters.

In Section 4, backed up by extensive empirical evaluation, we will systematically show that the local min-max training and the absolute value of the cosine similarity between the model loss gradients significantly improve the ensemble model robustness with negligible performance drop on benign accuracy, as well as reduce the adversarial transferability among base models.

3.2 TRS Training

We integrate the proposed TRS regularizer with the standard ensemble training loss, such as Ensemble Cross-Entropy (ECE) loss, to maintain both ensemble model’s classification utility and robustness by varying the balancing parameter λ_a and λ_b . Specifically, for an ensemble model consisting of N base models $\{\mathcal{F}_i\}_{i=1}^N$, given an input (x, y) , our final training loss train is defined as:

$$\mathcal{L}_{\text{train}} = \frac{1}{N} \sum_{i=1}^N \mathcal{L}_{\text{CE}}(\mathcal{F}_i(x), y) + \frac{2}{N(N-1)} \sum_{i=1}^N \sum_{j=i+1}^N \mathcal{L}_{\text{TRS}}(\mathcal{F}_i, \mathcal{F}_j, x, \delta)$$

where $\mathcal{L}_{\text{CE}}(\mathcal{F}_i(x), y)$ refers to the cross-entropy loss between $\mathcal{F}_i(x)$, the output vector of model \mathcal{F}_i given x , and the ground-truth label y . The weight of \mathcal{L}_{TRS} regularizer could be adjusted by the tuning λ_a and λ_b internally. We present one-epoch training pseudo code in Algorithm 1 of Appendix F. The detailed hyper-parameter setting and training criterion are discussed in Appendix F.

4 Experimental Evaluation

In this section, we evaluate the robustness of the proposed TRS-ensemble model under both strong whitebox attacks, as well as blackbox attacks considering the gradient obfuscation concern [1]. We compare TRS with six state-of-the-art ensemble approaches. In addition, we evaluate the adversarial transferability among base models within an ensemble and empirically show that the TRS regularizer can indeed reduce transferability effectively. We also conduct extensive ablation studies to explore the effectiveness of different loss terms in TRS, as well as visualize the trained decision boundaries of different ensemble models to provide intuition on the model properties. We open source the code³ and provide a large-scale benchmark.

4.1 Experimental Setup

Datasets. We conduct our experiments on widely-used image datasets including hand-written dataset MNIST [29]; and colourful image datasets CIFAR-10 and CIFAR-100 [26].

³<https://github.com/AI-secure/Transferability-Reduced-Smooth-Ensemble>

Table 1: Robust accuracy(%) of different ensembles against whitebox attacks on MNIST/CIFAR-10. “para.” refers to the attack parameter (ϵ is the ℓ_∞ perturbation budget for the attack and c the constant to balance the attack stealthiness and effectiveness). The first 6 methods are baseline ensembles, and the last 3 columns (Cos-only, Cos- ℓ_2 , TRS) the variants of TRS-ensemble.

MNIST	para.	AdaBoost	GradientBoost	CKAE	ADP	GAL	DVERGE	Cos-only	Cos- ℓ_2	TRS
FGSM	$\epsilon = 0.1$	70.2	73.2	72.6	71.7	35.7	95.8	66.2	91.2	95.6
	$\epsilon = 0.2$	39.4	34.2	42.5	20.0	7.8	91.6	30.7	72.5	91.7
BIM (50)	$\epsilon = 0.1$	2.6	2.4	4.2	7.7	4.6	74.9	0.4	76.2	93.3
	$\epsilon = 0.15$	0.0	0.2	0.4	0.1	2.5	47.7	0.0	47.9	85.7
PGD (50)	$\epsilon = 0.1$	1.9	1.5	1.4	4.5	4.1	69.2	0.0	73.4	93.0
	$\epsilon = 0.15$	0.0	0.0	0.5	1.0	0.6	28.8	0.0	30.2	85.1
MIM (50)	$\epsilon = 0.1$	1.9	1.6	1.2	13.8	0.8	75.3	0.4	74.1	92.9
	$\epsilon = 0.15$	0.0	0.1	0.3	1.0	0.2	44.6	0.0	35.5	85.1
CW	$c = 0.1$	81.2	80.5	83.4	97.9	97.4	97.3	85.6	89.2	98.1
	$c = 1.0$	66.3	65.8	69.5	90.1	68.3	79.2	58.6	54.4	92.6
EAD	$c = 5.0$	0.2	0.1	0.1	2.2	0.2	0.0	4.1	6.9	23.3
	$c = 10.0$	0.0	0.0	0.0	0.0	0.2	0.0	0.5	0.8	1.4
APGD-DLR	$\epsilon = 0.1$	0.5	0.2	0.5	2.1	1.9	65.4	0.0	70.6	92.1
	$\epsilon = 0.15$	0.0	0.0	0.1	0.5	0.2	27.4	0.0	26.3	83.4
APGD-CE	$\epsilon = 0.1$	0.2	0.2	0.1	1.4	1.2	63.2	0.0	69.8	91.7
	$\epsilon = 0.15$	0.0	0.0	0.1	0.4	0.2	26.1	0.0	25.4	82.8

CIFAR-10	para.	AdaBoost	GradientBoost	CKAE	ADP	GAL	DVERGE	Cos-only	Cos- ℓ_2	TRS
FGSM	$\epsilon = 0.02$	28.2	30.4	34.1	58.8	19.2	63.8	56.1	35.8	44.2
	$\epsilon = 0.04$	15.4	15.2	18.5	39.4	12.6	53.4	35.0	25.9	24.9
BIM (50)	$\epsilon = 0.01$	4.2	4.4	5.1	13.8	13.0	39.1	0.0	17.1	50.6
	$\epsilon = 0.02$	0.2	0.1	0.2	0.9	2.5	13.0	0.0	1.2	15.8
PGD (50)	$\epsilon = 0.01$	2.1	1.9	1.9	9.0	8.3	37.1	0.0	15.7	50.5
	$\epsilon = 0.02$	0.0	0.0	0.2	0.1	0.6	10.5	0.0	0.5	15.1
MIM (50)	$\epsilon = 0.01$	2.3	1.9	2.0	18.7	10.3	40.7	0.0	18.1	51.5
	$\epsilon = 0.02$	0.1	0.0	0.1	1.7	0.8	14.4	0.0	0.5	17.2
CW	$c = 0.01$	36.2	35.2	35.4	55.8	66.3	75.1	36.6	67.3	77.2
	$c = 0.1$	18.4	26.2	23.0	25.9	28.3	57.4	17.6	30.7	58.1
EAD	$c = 1.0$	0.2	0.0	0.0	9.0	0.0	0.2	0.0	0.0	11.7
	$c = 5.0$	0.0	0.0	0.0	0.0	0.0	0.0	0.0	0.0	0.1
APGD-DLR	$\epsilon = 0.01$	1.2	0.9	1.1	5.5	2.2	37.6	0.0	16.1	50.2
	$\epsilon = 0.02$	0.0	0.0	0.0	0.2	0.0	10.2	0.0	0.5	15.1
APGD-CE	$\epsilon = 0.01$	0.9	0.2	0.4	3.9	1.6	37.5	0.0	15.9	48.6
	$\epsilon = 0.02$	0.0	0.0	0.0	0.1	0.0	10.2	0.0	0.5	15.0

Baseline ensemble approaches. We mainly consider the standard ensemble, as well as the state-of-the-art robust ensemble methods that claim to be resilient against adversarial attacks. Specifically, we consider the following baseline ensemble methods which aim to promote the diversity between base models: **AdaBoost** [19]; **GradientBoost** [16]; **CKAE** [25]; **ADP** [38]; **GAL** [23]; **DVERGE** [56]. The detailed description about these approaches are in Appendix E. DVERGE, which has achieved the state-of-the-art ensemble robustness to our best knowledge, serves as the strongest baseline.

Whitebox robustness evaluation. We consider the following adversarial attacks to measure ensembles’ whitebox robustness: *Fast Gradient Sign Method (FGSM)* [17]; *Basic Iterative Method (BIM)* [34]; *Momentum Iterative Method (MIM)*; *Projected Gradient Descent (PGD)*; *Auto-PGD (APGD)*; *Carlini & Wanger Attack (CW)*; *Elastic-net Attack (EAD)* [8], and we leave the detailed description and parameter configuration of these attacks in Appendix E. We use *Robust Accuracy* as our **evaluation metric** for the whitebox setting, defined as the ratio of correctly predicted *adversarial examples* generated by different attacks among the whole test dataset.

Blackbox robustness evaluation. We also conduct blackbox robustness analysis in our evaluation since recent studies have shown that robust models which obfuscate gradients could still be fragile under blackbox attacks [1]. In the blackbox attack setting, we assume the attacker has no knowledge about the target ensemble, including the model architecture and parameters. In this case, the attacker is only able to craft adversarial examples based on several surrogate models and transfer them to the target victim ensemble. We follow the same blackbox attack evaluation setting in [56]: We choose three ensembles consisting of 3, 5, 8 base models which are trained with standard Ensemble Cross-Entropy (ECE) loss as our surrogate models. We apply 50-steps PGD attack with three random starts and two different loss functions (CrossEntropy and CW loss) on each surrogate model to generate adversarial instances (i.e. for each instance we will have 18 attack attempts). For each instance, among these attack attempts, as long as there is one that can successfully attack the victim model, we will count it as a successful attack. In this case, we use *Robust Accuracy* as our **evaluation metric**, defined as the number of unsuccessful attack attempts divided by the number of all attacks. We also consider additional three strong blackbox attacks targeting on reducing transferability (i.e., ILA [21], DI2-SGSM [55], IRA [50]) in Appendix J, which leads to similar observations.

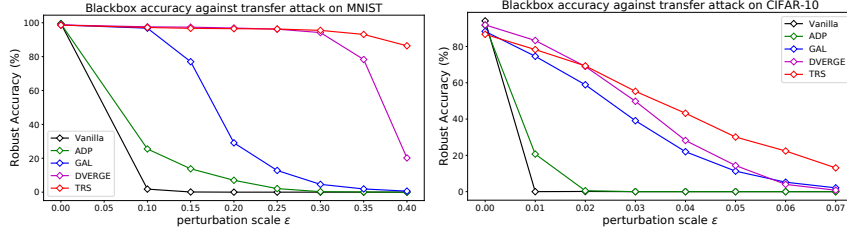


Figure 2: Robust accuracy under blackbox attacks with different ℓ_∞ perturbation budget ϵ . (Left): MNIST; (Right): CIFAR-10.

4.2 Experimental Results

In this section, we present both whitebox and blackbox robustness evaluation results, examine the adversarial transferability, and explore the impacts of different loss terms in TRS. Furthermore, in Appendix I.1, we visualize the decision boundary; in Appendix I.2, we show results of further improving the robustness of the TRS ensemble by integrating adversarial training; in Appendix I.3, we study the impacts of each of the regularization term \mathcal{L}_{sim} and $\mathcal{L}_{\text{smooth}}$; in Appendix I.4, we show the convergence of robust accuracy under large attack iterations to demonstrate the robustness stability of TRS ensemble; in Appendix I.5, we analyze the trade-off between the training cost and robustness of TRS by varying PGD step size and the total number of steps within $\mathcal{L}_{\text{smooth}}$ approximation.

Whitebox robustness. Table 1 presents the *Robust Accuracy* of different ensembles against a range of whitebox attacks on MNIST and CIFAR-100 dataset. We defer results on CIFAR-100 in Appendix K, and measure the statistical stability of our reported robust accuracy in Appendix H. Results shows that the proposed TRS ensemble outperforms other baselines including the state-of-the-art DVERGE *significantly*, against a range of attacks and perturbation budgets, and such performance gap could be even larger under stronger adversary attacks (e.g. PGD attack). We note that TRS ensemble is slightly less robust than DVERGE under small perturbation with weak attack FGSM. We investigate this based on the decision boundary analysis in Appendix I.1, and find that DVERGE tends to be more robust along the gradient direction and thus more robust against weak attacks which only focus on the gradient direction (e.g., FGSM); while TRS yields a smoother model along different directions leading to more consistent predictions within a larger neighborhood of an input, and thus more robust against strong iterative attacks (e.g., PGD). This may be due to that DVERGE is essentially performing adversarial training for different base models and therefore it protects the adversarial (gradient) direction, while TRS optimizes to train a smooth ensemble with diverse base models. We also analyze the convergence of attack algorithms in Appendix I.4, showing that when the number of attack iterations is large, both ADP and GAL ensemble achieve much lower robust accuracy against such iterative attacks; while both DVERGE and TRS remain robust.

Blackbox robustness. Figure 2 shows the *Robust Accuracy* performance of TRS compared with different baseline ensembles under different perturbation budget ϵ . As we can see, the TRS ensemble achieves competitive robust accuracy with DVERGE when ϵ is very small, and TRS beats *all* the baselines significantly when ϵ is large. Precisely speaking, TRS ensemble achieves over 85% robust accuracy against transfer attack with $\epsilon = 0.4$ on MNIST while the second-best ensemble (DVERGE) only achieves 20.2%. Also on CIFAR-10, TRS ensemble achieves over 25% robust accuracy against transfer attack when $\epsilon = 0.06$, while all the other baseline ensembles achieve robust accuracy lower than 6%. This implies that our proposed TRS ensemble has stronger generalization ability in terms of robustness against large ϵ adversarial attacks compared with other ensembles. We also put more details of the robust accuracy under blackbox attacks in Appendix G.

Adversarial transferability. Figure 3 shows the adversarial transferability matrix of different ensembles against 50-steps PGD attack with $\epsilon = 0.3$ for MNIST and $\epsilon = 0.04$ for CIFAR-10. Cell (i, j) where $i \neq j$ represents the transfer attack success rate evaluated on j -th base model by using the i -th base model as the surrogate model. Lower number in each cell indicates lower transferability and thus potentially higher ensemble robustness. The diagonal cell (i, i) refers to i -th base model’s attack success rate, which reflects the vulnerability of a single model. From these figures, we can see that while base models show their vulnerabilities against adversarial attack, only DVERGE and TRS ensemble could achieve low adversarial transferability among base models. We should also notice that though GAL applied a similar gradient cosine similarity loss as our loss term \mathcal{L}_{sim} , GAL still can

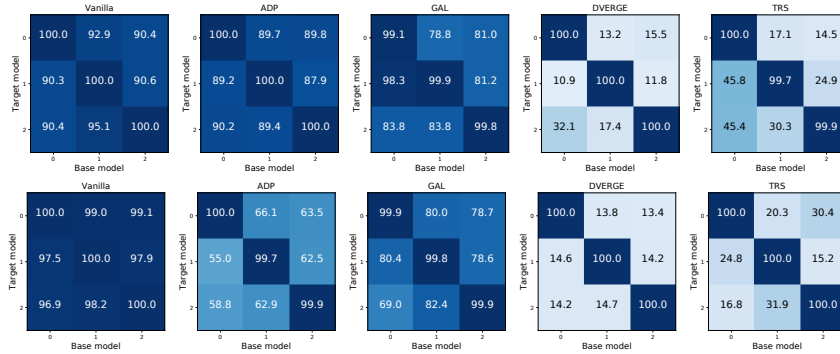


Figure 3: Transferability analysis of PGD attack on MNIST (top) and CIFAR-10 (bottom). Each cell (i, j) shows the *attack success rate* of i -th model on the adversarial examples generated against the j -th model. We use $\epsilon = 0.3$ for MNIST and $\epsilon = 0.04$ for CIFAR-10.

not achieve low adversarial transferability due to the lack of model smoothness enforcement, which is one of our key contributions in this paper.

Gradient similarity only vs. TRS. To further verify our theoretical analysis on the sufficient condition of transferability as model smoothness, we consider only applying *similarity loss* \mathcal{L}_{sim} without *model smoothness loss* $\mathcal{L}_{\text{smooth}}$ in TRS (i.e. $\lambda_b = 0$). The result is shown as “Cos-only” method of Table 1. We observe that the resulting whitebox robustness is much worse than standard TRS. This matches our theoretical analysis that *only minimizing the gradient similarity cannot guarantee low adversarial transferability among base models* and thus lead to low ensemble robustness. In Appendix I.3, we investigate the impacts of \mathcal{L}_{sim} and $\mathcal{L}_{\text{smooth}}$ thoroughly, and we show that though $\mathcal{L}_{\text{smooth}}$ contribute slightly more, both terms are critical to the final ensemble robustness.

ℓ_2 regularizer only vs. Min-max model smoothing. To emphasize the importance of our proposed min-max training loss on promoting the margin-wise model smoothness, we train a variant of TRS ensemble Cos- ℓ_2 , where we directly apply the ℓ_2 regularization on $\|\nabla_x \ell_{\mathcal{F}}\|_2$ and $\|\nabla_x \ell_{\mathcal{G}}\|_2$. The results are shown as “Cos- ℓ_2 ” in Table 1. We observe that Cos- ℓ_2 achieves lower robustness accuracy compared with TRS, which implies the necessity of regularizing the gradient magnitude on not only the local training points but also their neighborhood regions to ensure overall model smoothness.

5 Conclusion

In this paper, we deliver an in-depth understanding of adversarial transferability. Theoretically, we provide both lower and upper bounds on transferability which shows that *smooth* models together with *low loss gradient similarity* guarantee low transferability. Inspired by our analysis, we propose TRS ensemble training to empirically reduce transferability by reducing loss gradient similarity and promoting model smoothness, yielding a significant improvement on ensemble robustness.

Acknowledgments and Disclosure of Funding

This work is partially supported by the NSF grant No.1910100, NSF CNS 20-46726 CAR, the Amazon Research Award, and the joint CATCH MURI-AUSMURI.

References

- [1] Anish Athalye, Nicholas Carlini, and David Wagner. Obfuscated gradients give a false sense of security: Circumventing defenses to adversarial examples. In *International conference on machine learning*, pages 274–283. PMLR, 2018.
- [2] Jonathan Borwein and Adrian S Lewis. *Convex analysis and nonlinear optimization: theory and examples*. Springer Science & Business Media, 2010.
- [3] Stephen Boyd and Lieven Vandenberghe. *Convex Optimization*. Cambridge University Press, 2004.

- [4] Wieland Brendel, Jonas Rauber, and Matthias Bethge. Decision-based adversarial attacks: Reliable attacks against black-box machine learning models. In *International Conference on Learning Representations*, 2018.
- [5] Nicholas Carlini and David Wagner. Towards evaluating the robustness of neural networks. In *2017 IEEE Symposium on Security and Privacy (SP)*, pages 39–57. IEEE, 2017.
- [6] Nicholas Carlini, Anish Athalye, Nicolas Papernot, Wieland Brendel, Jonas Rauber, Dimitris Tsipras, Ian Goodfellow, Aleksander Madry, and Alexey Kurakin. On evaluating adversarial robustness. *arXiv preprint arXiv:1902.06705*, 2019.
- [7] Antonin Chambolle. An algorithm for total variation minimization and applications. *Journal of Mathematical imaging and vision*, 20(1):89–97, 2004.
- [8] Pin-Yu Chen, Yash Sharma, Huan Zhang, Jinfeng Yi, and Cho-Jui Hsieh. Ead: elastic-net attacks to deep neural networks via adversarial examples. In *Thirty-second AAAI conference on artificial intelligence*, 2018.
- [9] Shuyu Cheng, Yinpeng Dong, Tianyu Pang, Hang Su, and Jun Zhu. Improving black-box adversarial attacks with a transfer-based prior. In *Advances in Neural Information Processing Systems*, pages 10932–10942, 2019.
- [10] Sunoh Choi, Jangseong Bae, Changki Lee, Youngsoo Kim, and Jonghyun Kim. Attention-based automated feature extraction for malware analysis. *Sensors*, 20(10):2893, 2020.
- [11] Francesco Croce and Matthias Hein. Reliable evaluation of adversarial robustness with an ensemble of diverse parameter-free attacks. In *International conference on machine learning*, pages 2206–2216. PMLR, 2020.
- [12] Ambra Demontis, Marco Melis, Maura Pintor, Matthew Jagielski, Battista Biggio, Alina Oprea, Cristina Nita-Rotaru, and Fabio Roli. Why do adversarial attacks transfer? explaining transferability of evasion and poisoning attacks. In *28th USENIX Security Symposium (USENIX Security 19)*, pages 321–338, 2019.
- [13] Yinpeng Dong, Fangzhou Liao, Tianyu Pang, Hang Su, Jun Zhu, Xiaolin Hu, and Jianguo Li. Boosting adversarial attacks with momentum. In *Proceedings of the IEEE conference on computer vision and pattern recognition*, pages 9185–9193, 2018.
- [14] Harris Drucker and Yann Le Cun. Improving generalization performance using double back-propagation. *IEEE Transactions on Neural Networks*, 3(6):991–997, 1992.
- [15] Kevin Eykholt, Ivan Evtimov, Earlene Fernandes, Bo Li, Amir Rahmati, Chaowei Xiao, Atul Prakash, Tadayoshi Kohno, and Dawn Song. Robust physical-world attacks on deep learning visual classification. In *Proceedings of the IEEE Conference on Computer Vision and Pattern Recognition*, pages 1625–1634, 2018.
- [16] Jerome H Friedman. Greedy function approximation: a gradient boosting machine. *Annals of statistics*, pages 1189–1232, 2001.
- [17] Ian J Goodfellow, Jonathon Shlens, and Christian Szegedy. Explaining and harnessing adversarial examples. *arXiv preprint arXiv:1412.6572*, 2014.
- [18] Awni Hannun, Carl Case, Jared Casper, Bryan Catanzaro, Greg Diamos, Erich Elsen, Ryan Prenger, Sanjeev Satheesh, Shubho Sengupta, Adam Coates, et al. Deep speech: Scaling up end-to-end speech recognition. *arXiv preprint arXiv:1412.5567*, 2014.
- [19] Trevor Hastie, Saharon Rosset, Ji Zhu, and Hui Zou. Multi-class adaboost. *Statistics and its Interface*, 2(3):349–360, 2009.
- [20] Kaiming He, Xiangyu Zhang, Shaoqing Ren, and Jian Sun. Deep residual learning for image recognition. In *Proceedings of the IEEE conference on computer vision and pattern recognition*, pages 770–778, 2016.

- [21] Qian Huang, Isay Katsman, Horace He, Zeqi Gu, Serge Belongie, and Ser-Nam Lim. Enhancing adversarial example transferability with an intermediate level attack. In *Proceedings of the IEEE International Conference on Computer Vision*, pages 4733–4742, 2019.
- [22] Andrew Ilyas, Shibani Santurkar, Dimitris Tsipras, Logan Engstrom, Brandon Tran, and Aleksander Madry. Adversarial examples are not bugs, they are features. In *Advances in Neural Information Processing Systems*, pages 125–136, 2019.
- [23] Sanjay Kariyappa and Moinuddin K Qureshi. Improving adversarial robustness of ensembles with diversity training. *arXiv preprint arXiv:1901.09981*, 2019.
- [24] Diederik P. Kingma and Jimmy Ba. Adam: A method for stochastic optimization. In *Proceedings of 3rd International Conference for Learning Representations*, 2015.
- [25] Simon Kornblith, Mohammad Norouzi, Honglak Lee, and Geoffrey Hinton. Similarity of neural network representations revisited. In *International Conference on Machine Learning*, pages 3519–3529. PMLR, 2019.
- [26] Alex Krizhevsky, Geoffrey Hinton, et al. *Learning multiple layers of features from tiny images*. Citeseer, 2009.
- [27] Alex Krizhevsky, Ilya Sutskever, and Geoffrey E Hinton. ImageNet classification with deep convolutional neural networks. In *Advances in neural information processing systems*, pages 1097–1105, 2012.
- [28] Alexey Kurakin, Ian Goodfellow, and Samy Bengio. Adversarial examples in the physical world. *arXiv preprint arXiv:1607.02533*, 2016.
- [29] Yann LeCun. The mnist database of handwritten digits. <http://yann.lecun.com/exdb/mnist/>, 1998.
- [30] Huichen Li, Xiaojun Xu, Xiaolu Zhang, Shuang Yang, and Bo Li. Qeba: Query-efficient boundary-based blackbox attack. In *Proceedings of the IEEE/CVF Conference on Computer Vision and Pattern Recognition*, pages 1221–1230, 2020.
- [31] Huichen Li, Linyi Li, Xiaojun Xu, Xiaolu Zhang, Shuang Yang, and Bo Li. Nonlinear projection based gradient estimation for query efficient blackbox attacks. In *International Conference on Artificial Intelligence and Statistics*, pages 3142–3150. PMLR, 2021.
- [32] Yen-Chen Lin, Zhang-Wei Hong, Yuan-Hong Liao, Meng-Li Shih, Ming-Yu Liu, and Min Sun. Tactics of adversarial attack on deep reinforcement learning agents. In *Proceedings of the Twenty-Sixth International Joint Conference on Artificial Intelligence, IJCAI-17*, pages 3756–3762, 2017.
- [33] Yanpei Liu, Xinyun Chen, Chang Liu, and Dawn Song. Delving into transferable adversarial examples and black-box attacks. *arXiv preprint arXiv:1611.02770*, 2016.
- [34] Aleksander Madry, Aleksandar Makelov, Ludwig Schmidt, Dimitris Tsipras, and Adrian Vladu. Towards deep learning models resistant to adversarial attacks. In *International Conference on Learning Representations*, 2018.
- [35] Llew Mason, Jonathan Baxter, Peter Bartlett, and Marcus Frean. Boosting algorithms as gradient descent. *Advances in neural information processing systems*, 12:512–518, 1999.
- [36] Seyed-Mohsen Moosavi-Dezfooli, Alhussein Fawzi, Omar Fawzi, and Pascal Frossard. Universal adversarial perturbations. In *Proceedings of the IEEE conference on computer vision and pattern recognition*, pages 1765–1773, 2017.
- [37] Adam M Oberman and Jeff Calder. Lipschitz regularized deep neural networks converge and generalize. *arXiv preprint arXiv:1808.09540*, 2018.
- [38] Tianyu Pang, Kun Xu, Chao Du, Ning Chen, and Jun Zhu. Improving adversarial robustness via promoting ensemble diversity. In *International Conference on Machine Learning*, pages 4970–4979. PMLR, 2019.

- [39] Nicolas Papernot, Patrick McDaniel, and Ian Goodfellow. Transferability in machine learning: from phenomena to black-box attacks using adversarial samples. *arXiv preprint arXiv:1605.07277*, 2016.
- [40] Nicolas Papernot, Patrick McDaniel, Somesh Jha, Matt Fredrikson, Z Berkay Celik, and Ananthram Swami. The limitations of deep learning in adversarial settings. In *2016 IEEE European Symposium on Security and Privacy (EuroS&P)*, pages 372–387. IEEE, 2016.
- [41] Nicolas Papernot, Patrick McDaniel, Ian Goodfellow, Somesh Jha, Z Berkay Celik, and Ananthram Swami. Practical black-box attacks against deep learning systems using adversarial examples. In *Proceedings of the 2017 ACM Asia Conference on Computer and Communications Security*, 2017.
- [42] Nicolas Papernot, Patrick McDaniel, Ian Goodfellow, Somesh Jha, Z Berkay Celik, and Ananthram Swami. Practical black-box attacks against machine learning. In *Proceedings of the 2017 ACM on Asia Conference on Computer and Communications Security*, pages 506–519. ACM, 2017.
- [43] Robert E Schapire. The strength of weak learnability. *Machine learning*, 5(2):197–227, 1990.
- [44] Sahil Singla and Soheil Feizi. Second-order provable defenses against adversarial attacks. In *International Conference on Machine Learning*, 2020.
- [45] Aman Sinha, Hongseok Namkoong, and John Duchi. Certifying some distributional robustness with principled adversarial training. In *International Conference on Learning Representations*, 2018.
- [46] Ilya Sutskever, Oriol Vinyals, and Quoc V Le. Sequence to sequence learning with neural networks. In *Advances in neural information processing systems*, pages 3104–3112, 2014.
- [47] Christian Szegedy, Wojciech Zaremba, Ilya Sutskever, Joan Bruna, Dumitru Erhan, Ian Goodfellow, and Rob Fergus. Intriguing properties of neural networks. In *International Conference on Learning Representations*, 2014.
- [48] Florian Tramèr, Nicolas Papernot, Ian Goodfellow, Dan Boneh, and Patrick McDaniel. The space of transferable adversarial examples. *arXiv preprint arXiv:1704.03453*, 2017.
- [49] Florian Tramer, Nicholas Carlini, Wieland Brendel, and Aleksander Madry. On adaptive attacks to adversarial example defenses. *Advances in Neural Information Processing Systems*, 33, 2020.
- [50] Xin Wang, Jie Ren, Shuyun Lin, Xiangming Zhu, Yisen Wang, and Quanshi Zhang. A unified approach to interpreting and boosting adversarial transferability. In *International Conference on Learning Representations*, 2020.
- [51] Chaowei Xiao, Bo Li, Jun-Yan Zhu, Warren He, Mingyan Liu, and Dawn Song. Generating adversarial examples with adversarial networks. In *Proceedings of the 27th International Joint Conference on Artificial Intelligence*, pages 3905–3911, 2018.
- [52] Chaowei Xiao, Bo Li, Jun-Yan Zhu, Warren He, Mingyan Liu, and Dawn Song. Generating adversarial examples with adversarial networks. In *Proceedings of the 27th International Joint Conference on Artificial Intelligence*, pages 3905–3911, 2018.
- [53] Chaowei Xiao, Jun-Yan Zhu, Bo Li, Warren He, Mingyan Liu, and Dawn Song. Spatially transformed adversarial examples. In *International Conference on Learning Representations*, 2018.
- [54] Chaowei Xiao, Jun Yan Zhu, Bo Li, Warren He, Mingyan Liu, and Dawn Song. Spatially transformed adversarial examples. In *6th International Conference on Learning Representations, ICLR 2018*, 2018.
- [55] Cihang Xie, Zhishuai Zhang, Yuyin Zhou, Song Bai, Jianyu Wang, Zhou Ren, and Alan L Yuille. Improving transferability of adversarial examples with input diversity. In *Proceedings of the IEEE/CVF Conference on Computer Vision and Pattern Recognition*, pages 2730–2739, 2019.

- [56] Huanrui Yang, Jingyang Zhang, Hongliang Dong, Nathan Inkawich, Andrew Gardner, Andrew Touchet, Wesley Wilkes, Heath Berry, and Hai Li. Dverge: Diversifying vulnerabilities for enhanced robust generation of ensembles. *Advances in Neural Information Processing Systems*, 33, 2020.
- [57] Jiawei Zhang, Linyi Li, Huichen Li, Xiaolu Zhang, Shuang Yang, and Bo Li. Progressive-scale boundary blackbox attack via projective gradient estimation. *arXiv preprint arXiv:2106.06056*, 2021.

Checklist

1. For all authors...
 - (a) Do the main claims made in the abstract and introduction accurately reflect the paper’s contributions and scope? [Yes]
 - (b) Did you describe the limitations of your work? [Yes]
 - (c) Did you discuss any potential negative societal impacts of your work? [Yes]
 - (d) Have you read the ethics review guidelines and ensured that your paper conforms to them? [Yes]
2. If you are including theoretical results...
 - (a) Did you state the full set of assumptions of all theoretical results? [Yes]
 - (b) Did you include complete proofs of all theoretical results? [Yes]
3. If you ran experiments...
 - (a) Did you include the code, data, and instructions needed to reproduce the main experimental results (either in the supplemental material or as a URL)? [Yes]
 - (b) Did you specify all the training details (e.g., data splits, hyperparameters, how they were chosen)? [Yes]
 - (c) Did you report error bars (e.g., with respect to the random seed after running experiments multiple times)? [Yes]
 - (d) Did you include the total amount of compute and the type of resources used (e.g., type of GPUs, internal cluster, or cloud provider)? [Yes]
4. If you are using existing assets (e.g., code, data, models) or curating/releasing new assets...
 - (a) If your work uses existing assets, did you cite the creators? [Yes]
 - (b) Did you mention the license of the assets? [Yes]
 - (c) Did you include any new assets either in the supplemental material or as a URL? [Yes]
 - (d) Did you discuss whether and how consent was obtained from people whose data you’re using/curating? [Yes]
 - (e) Did you discuss whether the data you are using/curating contains personally identifiable information or offensive content? [Yes]
5. If you used crowdsourcing or conducted research with human subjects...
 - (a) Did you include the full text of instructions given to participants and screenshots, if applicable? [N/A]
 - (b) Did you describe any potential participant risks, with links to Institutional Review Board (IRB) approvals, if applicable? [N/A]
 - (c) Did you include the estimated hourly wage paid to participants and the total amount spent on participant compensation? [N/A]

In Appendix A, we provide the lower and upper bounds of attack transferability for untargeted attacks. In Appendix B, we extend our theoretical analysis to adversarial attacks bounded by distributional distance. In Appendices C and D, we give the detailed proof of Theorems 1, 2, 3 and 4 characterizing the lower and upper bounds for both targeted and untargeted attack transferability. In Appendix E, we give the detailed introduction of our baseline ensembles and evaluated whitebox attacks, including their exact configuration. In Appendix F, we present all the training details for TRS ensemble and other baselines. In Appendix G, we give the numerical blackbox robustness evaluation results on MNIST and CIFAR-10, corresponding to Figure 2 in main paper. In Appendix H, we analyze the statistical stability of reported robust accuracy for TRS ensemble against attacks with random start, and TRS ensemble claims its stability by showing small standard deviation. In Appendix I, we visualize the decision boundaries of different robust ensembles and investigate how adversarial training would further improve the robustness of TRS ensemble. We also show TRS ensemble remains robust under large attack iterations through convergence analysis. In Appendix J, we evaluate the robustness of TRS ensemble against other three strong blackbox attacks, and TRS ensemble still remains robust. In Appendix K, we conduct whitebox robustness evaluation on CIFAR-100 dataset and compare other state-of-the-art robust ensembles with our proposed TRS ensemble.

A Additional Theoretical Results for Untargeted Attacks

In this appendix, we present transferability lower and upper bounds for untargeted attack. All these bounds have similar forms as their targeted attack counterparts in the main text.

A.1 Lower Bound

Theorem 3 (Lower Bound on Untargeted Attack Transferability). *Assume both models \mathcal{F} and \mathcal{G} are β -smooth. Let \mathcal{A}_U be an (α, \mathcal{F}) -effective untargeted attack with perturbation ball $\|\delta\|_2 \leq \epsilon$. The transferability can be lower bounded by*

$$\Pr(T_r(\mathcal{F}, \mathcal{G}, x) = 1) \geq (1 - \alpha) - (\eta_{\mathcal{F}} + \eta_{\mathcal{G}}) - \frac{\epsilon(1 + \alpha) - c_{\mathcal{F}}(1 - \alpha)}{\epsilon - c_{\mathcal{G}}} - \frac{\epsilon(1 - \alpha)}{\epsilon - c_{\mathcal{G}}} \sqrt{2 - 2\mathcal{S}(\ell_{\mathcal{F}}, \ell_{\mathcal{G}})},$$

where

$$c_{\mathcal{F}} = \min_{(x, y) \in \text{supp}(\mathcal{D})} \frac{\min_{y' \in \mathcal{Y}: y' \neq y} \ell_{\mathcal{F}}(\mathcal{A}_U(x), y') - \ell_{\mathcal{F}}(x, y) - \beta\epsilon^2/2}{\|\nabla_x \ell_{\mathcal{F}}(x, y)\|_2}, c_{\mathcal{G}} = \max_{(x, y) \in \text{supp}(\mathcal{D})} \frac{\min_{y' \in \mathcal{Y}: y' \neq y} \ell_{\mathcal{G}}(\mathcal{A}_U(x), y') - \ell_{\mathcal{G}}(x, y) + \beta\epsilon^2/2}{\|\nabla_x \ell_{\mathcal{G}}(x, y)\|_2}.$$

Here $\eta_{\mathcal{F}}$ and $\eta_{\mathcal{G}}$ are the risks of models \mathcal{F} and \mathcal{G} respectively. The $\text{supp}(\mathcal{D})$ is the support of benign data distribution, i.e., x is the benign data and y is its associated true label.

The full proof is available in Appendix C. The discussion of the theorem is in Section 2.

A.2 Upper Bound

Theorem 4 (Upper Bound on Untargeted Attack Transferability). *Assume both models \mathcal{F} and \mathcal{G} are β -smooth with gradient magnitude bounded by B , i.e., $\|\nabla_x \ell_{\mathcal{F}}(x, y)\| \leq B$ and $\|\nabla_x \ell_{\mathcal{G}}(x, y)\| \leq B$ for any $x \in \mathcal{X}$, $y \in \mathcal{Y}$. Let \mathcal{A}_U be an (α, \mathcal{F}) -effective untargeted attack with perturbation ball $\|\delta\|_2 \leq \epsilon$. When the attack radius ϵ is small such that $\ell_{\min} - \epsilon B \left(1 + \sqrt{\frac{1 + \mathcal{S}(\ell_{\mathcal{F}}, \ell_{\mathcal{G}})}{2}}\right) - \beta\epsilon^2 > 0$, the transferability can be upper bounded by*

$$\Pr(T_r(\mathcal{F}, \mathcal{G}, x) = 1) \leq \frac{\xi_{\mathcal{F}} + \xi_{\mathcal{G}}}{\ell_{\min} - \epsilon B \left(1 + \sqrt{\frac{1 + \mathcal{S}(\ell_{\mathcal{F}}, \ell_{\mathcal{G}})}{2}}\right) - \beta\epsilon^2},$$

where $\ell_{\min} = \min_{\substack{x \in \mathcal{X}, y' \in \mathcal{Y}: \\ (x, y) \in \text{supp}(\mathcal{D}), y' \neq y}} (\ell_{\mathcal{F}}(x, y'), \ell_{\mathcal{G}}(x, y'))$. Here $\xi_{\mathcal{F}}$ and $\xi_{\mathcal{G}}$ are the empirical risks of

models \mathcal{F} and \mathcal{G} respectively, defined relative to a differentiable loss. The $\text{supp}(\mathcal{D})$ is the support of benign data distribution, i.e., x is the benign data and y is its associated true label.

The full proof is available in Appendix D. The discussion of the theorem is in Section 2.

B Discussion: Beyond ℓ_p Attack

Besides the widely used ℓ_p norm based adversarial examples, here we plan to extend our understanding to the distribution distance analysis.

We no longer distinguish the targeted attack and untargeted attack. Therefore, we denote either of them by \mathcal{A} . Accordingly, we revise the definition of (α, \mathcal{F}) -effective attack (Definition 2) to be $\Pr(\mathcal{F}(\mathcal{A}(x)) \neq y) \geq 1 - \alpha$ where $y \in \mathcal{Y}$ is the true label of $x \in \mathcal{X}$.

Moreover, we use $\mathcal{P}_{\mathcal{A}(x)}$ to represent the distribution of $\mathcal{A}(x) \in \mathcal{X}$ where x is distributed according to $\mathcal{P}_{\mathcal{X}}$.

Now we define the distribution distance that we use to measure the adversarial distribution gap.

Definition 7 (Total variation distance; [7]). *For two probability distributions $\mathcal{P}_{\mathcal{X}}$ and $\mathcal{P}_{\mathcal{A}(x)}$ on \mathcal{X} , the total variation distance between them is defined as*

$$\|\mathcal{P}_{\mathcal{X}} - \mathcal{P}_{\mathcal{A}(x)}\|_{TV} = \sup_{C \subseteq \mathcal{X}} |\mathcal{P}_{\mathcal{X}}(C) - \mathcal{P}_{\mathcal{A}(x)}(C)|.$$

Informally, the total variation distance measures the largest change in probability over all events. For discrete probability distributions, the total variation distance is the ℓ_1 distance between the vectors in the probability simplex representing the two distributions.

Definition 8. *Given $\rho \in (0, 1)$, an attack strategy $\mathcal{A}(\cdot)$ is called ρ -conservative, if for $x \sim \mathcal{P}_{\mathcal{X}}$, $\|\mathcal{P}_{\mathcal{X}} - \mathcal{P}_{\mathcal{A}(x)}\|_{TV} \leq \rho$.*

This definition formalizes the general objective of generating adversarial examples against deep neural networks: attack samples are likely to be observed, while they do not themselves arouse suspicion.

Lemma 5. *Let $f, g : \mathcal{X} \rightarrow \mathcal{Y}$ be classifiers, $\delta, \rho, \epsilon \in (0, 1)$ be constants, and $\mathcal{A}(\cdot)$ be an attack strategy. Suppose that $\mathcal{A}(\cdot)$ is ρ -conservative and f, g have risk at most ϵ . Then*

$$\Pr(\mathcal{F}(\mathcal{A}(x)) \neq \mathcal{G}(\mathcal{A}(x))) \leq 2\epsilon + \rho$$

for a given random instance $x \sim \mathcal{P}_{\mathcal{X}}$.

Remark. This result provides theoretical backing for the intuition that the boundaries of low risk classifiers under certain dense data distribution are close [48]. It considers two classifiers that have risk at most ϵ , which indicates their boundaries are close for benign data. It then shows that their boundaries are also close for the perturbed data as long as the attack strategy satisfies a conservative condition which constrains the drift in distribution between the benign and adversarial data.

Proof of Lemma 5. Given $\mathcal{A}(\cdot)$ is ρ -conservative, by Definition 8 we know

$$\begin{aligned} & |\Pr_{\mathcal{P}_{\mathcal{X}}}(f(\mathcal{A}(x)) = g(\mathcal{A}(x))) - \Pr_{\mathcal{X}}(f(x) = g(x))| \\ &= |\Pr_{\mathcal{A}(x)}(f(x) = g(x)) - \Pr_{\mathcal{X}}(f(x) = g(x))| \\ &\leq \rho. \end{aligned}$$

Therefore, we have

$$\Pr(f(\mathcal{A}(x)) = g(\mathcal{A}(x))) \geq \Pr(f(x) = g(x)) - \rho.$$

From the low-risk conditions, the classifiers agree with high probability:

$$\begin{aligned} & \Pr(f(\mathcal{A}(x)) \neq g(\mathcal{A}(x))) \\ &\leq \Pr(f(x) \neq g(x)) + \rho \\ &\leq 1 - \Pr(f(x) = y, g(x) = y) + \rho, \quad ^4 \\ &\leq 1 - (1 - \Pr(f(x) \neq y) - \Pr(g(x) \neq y)) + \rho \\ &= \epsilon + \epsilon + \rho \\ &\leq 2\epsilon + \rho, \end{aligned}$$

where the third inequality follows from the union bound. ⁵ □

⁴Here we assume y is the ground truth label.

⁵Recall that for arbitrary events A_1, \dots, A_n , the union bound implies $P(\bigcap_{i=1}^n A_i) \geq 1 - \sum_{i=1}^n P(\bar{A}_i)$.

Theorem 6. Let $\mathcal{F}, \mathcal{G} : \mathcal{X} \rightarrow \mathcal{Y}$ be classifiers ($\mathcal{Y} \in \{-1, 1\}$), $\delta, \rho, \epsilon \in (0, 1)$ be constants, and $\mathcal{A}(\cdot)$ an attack strategy. Suppose that $\mathcal{A}(\cdot)$ is ρ -conservative and \mathcal{F}, \mathcal{G} have risk at most ϵ . Given random instance $x \in \mathcal{X}$, if $\mathcal{A}(\cdot)$ is (δ, \mathcal{F}) -effective, then it is also $(\delta + 2\epsilon + \rho, \mathcal{G})$ -effective.

The proof is shown below. This result formalizes the intuition that low-risk classifiers possess close decision boundaries in high-probability regions. In such settings, an attack strategy that successfully attacks one classifier would have high probability to mislead the other. This theorem explains why we should expect successful transferability in practice: defenders will naturally prefer low-risk binary classifiers. This desirable quality of classifiers is a potential liability.

Proof of Theorem 6. From Lemma 5 and the union bound we have

$$\begin{aligned} & \Pr(g(x) \neq y) \\ & \geq \Pr(f(\mathcal{A}(x)) \neq y, g(\mathcal{A}(x)) = f(\mathcal{A}(x))) \\ & \geq 1 - \Pr(f(\mathcal{A}(x)) = y) - \Pr(g(\mathcal{A}(x)) \neq f(\mathcal{A}(x))) \\ & \geq 1 - \delta - 2\epsilon - \rho, \end{aligned}$$

as claimed. \square

C Proof of Transferability Lower Bound (Theorems 1 and 3)

Here we present the proof of Theorem 1 and Theorem 3 stated in Section 2.3 and Appendix A.

The following lemma is used in the proof.

Lemma 7. For arbitrary vector δ , x, y , suppose $\|\delta\|_2 \leq \epsilon$, x and y are unit vectors, i.e., $\|x\|_2 = \|y\|_2 = 1$. Let $m := \cos\langle x, y \rangle = \frac{x \cdot y}{\|x\|_2 \cdot \|y\|_2}$. Let c denote any real number. Then

$$\delta \cdot y > c + \epsilon\sqrt{2 - 2m} \Rightarrow \delta \cdot x > c.$$

Proof. $\delta \cdot x = \delta \cdot y + \delta \cdot (x - y) > c + \epsilon\sqrt{2 - 2m} + \delta \cdot (x - y)$. By law of cosines, $\delta \cdot (x - y) \geq -\epsilon\sqrt{2 - 2\cos\langle x, y \rangle} = -\epsilon\sqrt{2 - 2m}$. Hence, $\delta \cdot x > c$. \square

Theorem (Lower Bound on Targeted Attack Transferability). Assume both models \mathcal{F} and \mathcal{G} are β -smooth. Let \mathcal{A}_T be an (α, \mathcal{F}) -effective targeted attack with perturbation ball $\|\delta\|_2 \leq \epsilon$ and target label $y_t \in \mathcal{Y}$. The transferability can be lower bounded by

$$\Pr(T_r(\mathcal{F}, \mathcal{G}, x, y_t) = 1) \geq (1 - \alpha) - (\eta_{\mathcal{F}} + \eta_{\mathcal{G}}) - \frac{\epsilon(1 + \alpha) + c_{\mathcal{F}}(1 - \alpha)}{c_{\mathcal{G}} + \epsilon} - \frac{\epsilon(1 - \alpha)}{c_{\mathcal{G}} + \epsilon} \sqrt{2 - 2\underline{\mathcal{S}}(\ell_{\mathcal{F}}, \ell_{\mathcal{G}})},$$

where

$$\begin{aligned} c_{\mathcal{F}} &= \max_{x \in \mathcal{X}} \frac{\min_{y \in \mathcal{Y}} \ell_{\mathcal{F}}(\mathcal{A}_T(x), y) - \ell_{\mathcal{F}}(x, y_t) + \beta\epsilon^2/2}{\|\nabla_x \ell_{\mathcal{F}}(x, y_t)\|_2}, \\ c_{\mathcal{G}} &= \min_{x \in \mathcal{X}} \frac{\min_{y \in \mathcal{Y}} \ell_{\mathcal{G}}(\mathcal{A}_T(x), y) - \ell_{\mathcal{G}}(x, y_t) - \beta\epsilon^2/2}{\|\nabla_x \ell_{\mathcal{G}}(x, y_t)\|_2}. \end{aligned}$$

Here $\eta_{\mathcal{F}}, \eta_{\mathcal{G}}$ are the risks of models \mathcal{F} and \mathcal{G} respectively.

Proof. For simplifying the notations, we define $x^{\mathcal{A}} := \mathcal{A}_T(x)$, which is the generated adversarial example by \mathcal{A}_T when the input is x .

Define auxiliary function $f, g : \mathcal{X} \mapsto \mathbb{R}$ such that

$$\begin{aligned} f(x) &= \frac{\min_{y \in \mathcal{Y}} \ell_{\mathcal{F}}(x^{\mathcal{A}}, y) - \ell_{\mathcal{F}}(x, y_t) + \beta\epsilon^2/2}{\|\nabla_x \ell_{\mathcal{F}}(x, y_t)\|_2}, \\ g(x) &= \frac{\min_{y \in \mathcal{Y}} \ell_{\mathcal{G}}(x^{\mathcal{A}}, y) - \ell_{\mathcal{G}}(x, y_t) - \beta\epsilon^2/2}{\|\nabla_x \ell_{\mathcal{G}}(x, y_t)\|_2}. \end{aligned}$$

The f and g are orthogonal to the confidence score functions of model \mathcal{F} and \mathcal{G} . Note that $c_{\mathcal{F}} = \max_{x \in \mathcal{X}} f(x)$ and $c_{\mathcal{G}} = \min_{x \in \mathcal{X}} g(x)$.

The transferability of concern satisfies:

$$\begin{aligned} & \Pr(T_r(\mathcal{F}, \mathcal{G}, x, y_t) = 1) \\ &= \Pr(\mathcal{F}(x) = y \cap \mathcal{G}(x) = y \cap \mathcal{F}(x^A) = y_t \cap \mathcal{G}(x^A) = y_t) \end{aligned} \quad (2)$$

$$\geq 1 - \Pr(\mathcal{F}(x) \neq y) - \Pr(\mathcal{G}(x) \neq y) - \Pr(\mathcal{F}(x^A) \neq y_t) - \Pr(\mathcal{G}(x^A) \neq y_t) \quad (3)$$

$$\geq 1 - \eta_{\mathcal{F}} - \eta_{\mathcal{G}} - \alpha - \Pr(\mathcal{G}(x^A) \neq y_t). \quad (4)$$

Eq. 2 follows the definition (Definition 6). Eq. 2 to Eq. 3 follows from the union bound. From Eq. 2 to Eq. 3 definition of model risk (Definition 3) and definition of adversarial effectiveness (Definition 2) are applied.

Now consider $\Pr(\mathcal{F}(x^A) \neq y_t)$ and $\Pr(\mathcal{G}(x^A) \neq y_t)$. Given that model predicts the label for which $\ell_{\mathcal{F}}$ is minimized, $\mathcal{F}(x^A) \neq y_t \iff \ell_{\mathcal{F}}(x + \delta, y_t) > \min_y \ell_{\mathcal{F}}(x + \delta, y)$. Similarly, $\mathcal{G}(x^A) \neq y_t \iff \ell_{\mathcal{G}}(x + \delta, y_t) > \min_y \ell_{\mathcal{G}}(x + \delta, y)$.

Following Taylor's Theorem with Lagrange remainder, we have

$$\ell_{\mathcal{F}}(x + \delta, y_t) = \ell_{\mathcal{F}}(x, y_t) + \delta \nabla_x \ell_{\mathcal{F}}(x, y_t) + \frac{1}{2} \xi^\top \mathbf{H}_{\mathcal{F}} \xi, \quad (5)$$

$$\ell_{\mathcal{G}}(x + \delta, y_t) = \ell_{\mathcal{G}}(x, y_t) + \delta \nabla_x \ell_{\mathcal{G}}(x, y_t) + \frac{1}{2} \xi^\top \mathbf{H}_{\mathcal{G}} \xi. \quad (6)$$

In Eq. 5 and Eq. 6, $\xi = k\delta$ for some $k \in [0, 1]$. $\mathbf{H}_{\mathcal{F}}$ and $\mathbf{H}_{\mathcal{G}}$ are Hessian matrices of $\ell_{\mathcal{F}}$ and $\ell_{\mathcal{G}}$ respectively. Since $\ell_{\mathcal{F}}(x + \delta, y_t)$ and $\ell_{\mathcal{G}}(x + \delta, y_t)$ are β -smooth, the maximum eigenvalues of $\mathbf{H}_{\mathcal{F}}$ and $\mathbf{H}_{\mathcal{G}}$ are bounded by β . As the result, $|\xi^\top \mathbf{H}_{\mathcal{F}} \xi| \leq \beta \cdot \|\xi\|_2^2 \leq \beta \epsilon^2$. Applying them to Eq. 5 and Eq. 6, we thus have

$$\ell_{\mathcal{F}}(x, y_t) + \delta \nabla_x \ell_{\mathcal{F}}(x, y_t) - \frac{1}{2} \beta \epsilon^2 \leq \ell_{\mathcal{F}}(x + \delta, y_t) \leq \ell_{\mathcal{F}}(x, y_t) + \delta \nabla_x \ell_{\mathcal{F}}(x, y_t) + \frac{1}{2} \beta \epsilon^2, \quad (7)$$

$$\ell_{\mathcal{G}}(x, y_t) + \delta \nabla_x \ell_{\mathcal{G}}(x, y_t) - \frac{1}{2} \beta \epsilon^2 \leq \ell_{\mathcal{G}}(x + \delta, y_t) \leq \ell_{\mathcal{G}}(x, y_t) + \delta \nabla_x \ell_{\mathcal{G}}(x, y_t) + \frac{1}{2} \beta \epsilon^2. \quad (8)$$

Apply left hand side of Eq. 7 to $\Pr(\mathcal{F}(x^A) \neq y_t) \leq \alpha$ (from Definition 2):

$$\begin{aligned} & \Pr(\mathcal{F}(x^A) \neq y_t) \\ &= \Pr\left(\ell_{\mathcal{F}}(x + \delta, y_t) > \min_y \ell_{\mathcal{F}}(x + \delta, y)\right) \\ &\geq \Pr\left(\ell_{\mathcal{F}}(x, y_t) + \delta \nabla_x \ell_{\mathcal{F}}(x, y_t) - \frac{1}{2} \beta \epsilon^2 > \min_y \ell_{\mathcal{F}}(x + \delta, y)\right) \\ &= \Pr\left(\delta \cdot \frac{\nabla_x \ell_{\mathcal{F}}(x, y_t)}{\|\nabla_x \ell_{\mathcal{F}}(x, y_t)\|_2} > f(x)\right), \\ &\implies \Pr\left(\delta \cdot \frac{\nabla_x \ell_{\mathcal{F}}(x, y_t)}{\|\nabla_x \ell_{\mathcal{F}}(x, y_t)\|_2} > f(x)\right) \leq \alpha. \end{aligned}$$

Similarly, we apply right hand side of Eq. 8 to $\Pr(\mathcal{G}(x^A) = y_t)$:

$$\begin{aligned} & \Pr(\mathcal{G}(x^A) \neq y_t) \\ &= \Pr\left(\ell_{\mathcal{G}}(x + \delta, y_t) > \min_y \ell_{\mathcal{G}}(x + \delta, y)\right) \\ &\leq \Pr\left(\ell_{\mathcal{G}}(x, y_t) + \delta \nabla_x \ell_{\mathcal{G}}(x, y_t) + \frac{1}{2} \beta \epsilon^2 > \min_y \ell_{\mathcal{G}}(x + \delta, y)\right) \\ &= \Pr\left(\delta \cdot \frac{\nabla_x \ell_{\mathcal{G}}(x, y_t)}{\|\nabla_x \ell_{\mathcal{G}}(x, y_t)\|_2} > g(x)\right). \end{aligned} \quad (9)$$

Knowing that $\|\delta\|_2 \leq \epsilon$, from Lemma 7 we have

$$\delta \cdot \frac{\nabla_x \ell_{\mathcal{G}}(x, y_t)}{\|\nabla_x \ell_{\mathcal{G}}(x, y_t)\|_2} > f(x) + \epsilon \sqrt{2 - 2\underline{\mathcal{S}}(\ell_{\mathcal{F}}, \ell_{\mathcal{G}})} \quad (10)$$

$$\implies \delta \cdot \frac{\nabla_x \ell_{\mathcal{G}}(x, y_t)}{\|\nabla_x \ell_{\mathcal{G}}(x, y_t)\|_2} > f(x) + \epsilon \sqrt{2 - 2 \cos \langle \nabla_x \ell_{\mathcal{F}}(x, y_t), \nabla_x \ell_{\mathcal{G}}(x, y_t) \rangle} \quad (11)$$

$$\implies \delta \cdot \frac{\nabla_x \ell_{\mathcal{F}}(x, y_t)}{\|\nabla_x \ell_{\mathcal{F}}(x, y_t)\|_2} > f(x). \quad (12)$$

From Eq. 10 to Eq. 11, the infimum in definition of $\underline{\mathcal{S}}$ (Definition 4) indicates that

$$\underline{\mathcal{S}}(\ell_{\mathcal{F}}, \ell_{\mathcal{G}}) \leq \cos \langle \nabla_x \ell_{\mathcal{F}}(x, y_t), \nabla_x \ell_{\mathcal{G}}(x, y_t) \rangle.$$

Hence,

$$f(x) + \epsilon \sqrt{2 - 2 \underline{\mathcal{S}}(\ell_{\mathcal{F}}, \ell_{\mathcal{G}})} \geq f(x) + \epsilon \sqrt{2 - 2 \cos \langle \nabla_x \ell_{\mathcal{F}}(x, y_t), \nabla_x \ell_{\mathcal{G}}(x, y_t) \rangle}.$$

Eq. 11 to Eq. 12 directly uses Lemma 7. As a result,

$$\begin{aligned} & \Pr \left(\delta \cdot \frac{\nabla_x \ell_{\mathcal{G}}(x, y_t)}{\|\nabla_x \ell_{\mathcal{G}}(x, y_t)\|_2} > f(x) + \epsilon \sqrt{2 - 2 \underline{\mathcal{S}}(\ell_{\mathcal{F}}, \ell_{\mathcal{G}})} \right) \\ & \leq \Pr \left(\delta \cdot \frac{\nabla_x \ell_{\mathcal{F}}(x, y_t)}{\|\nabla_x \ell_{\mathcal{F}}(x, y_t)\|_2} > f(x) \right) \leq \alpha. \end{aligned}$$

Note that $f(x) \leq c_{\mathcal{F}}$, we have

$$\Pr \left(\delta \cdot \frac{\nabla_x \ell_{\mathcal{G}}(x, y_t)}{\|\nabla_x \ell_{\mathcal{G}}(x, y_t)\|_2} > c_{\mathcal{F}} + \epsilon \sqrt{2 - 2 \underline{\mathcal{S}}(\ell_{\mathcal{F}}, \ell_{\mathcal{G}})} \right) \leq \alpha.$$

Now we consider the maximum expectation of $\delta \cdot \frac{\nabla_x \ell_{\mathcal{G}}(x, y_t)}{\|\nabla_x \ell_{\mathcal{G}}(x, y_t)\|_2}$. Its maximum is $\max \|\delta\|_2 = \epsilon$. Therefore, its expectation is bounded:

$$\mathbb{E} \left[\delta \cdot \frac{\nabla_x \ell_{\mathcal{G}}(x, y_t)}{\|\nabla_x \ell_{\mathcal{G}}(x, y_t)\|_2} \right] \leq \epsilon \cdot \alpha + \left(c_{\mathcal{F}} + \epsilon \sqrt{2 - 2 \underline{\mathcal{S}}(\ell_{\mathcal{F}}, \ell_{\mathcal{G}})} \right) (1 - \alpha).$$

Now applying Markov's inequality, we get

$$\begin{aligned} & \Pr \left(\delta \cdot \frac{\nabla_x \ell_{\mathcal{G}}(x, y_t)}{\|\nabla_x \ell_{\mathcal{G}}(x, y_t)\|_2} > c_{\mathcal{G}} \right) \\ & \leq \frac{\epsilon \cdot \alpha + \left(c_{\mathcal{F}} + \epsilon \sqrt{2 - 2 \underline{\mathcal{S}}(\ell_{\mathcal{F}}, \ell_{\mathcal{G}})} \right) (1 - \alpha) + \epsilon}{c_{\mathcal{G}} + \epsilon} \\ & = \frac{\epsilon(1 + \alpha) + \left(c_{\mathcal{F}} + \epsilon \sqrt{2 - 2 \underline{\mathcal{S}}(\ell_{\mathcal{F}}, \ell_{\mathcal{G}})} \right) (1 - \alpha)}{c_{\mathcal{G}} + \epsilon}. \end{aligned}$$

Since $g(x) \geq c_{\mathcal{G}}$,

$$\begin{aligned} & \Pr \left(\delta \cdot \frac{\nabla_x \ell_{\mathcal{G}}(x, y_t)}{\|\nabla_x \ell_{\mathcal{G}}(x, y_t)\|_2} > g(x) \right) \leq \Pr \left(\delta \cdot \frac{\nabla_x \ell_{\mathcal{G}}(x, y_t)}{\|\nabla_x \ell_{\mathcal{G}}(x, y_t)\|_2} > c_{\mathcal{G}} \right) \\ & \leq \frac{\epsilon(1 + \alpha) + \left(c_{\mathcal{F}} + \epsilon \sqrt{2 - 2 \underline{\mathcal{S}}(\ell_{\mathcal{F}}, \ell_{\mathcal{G}})} \right) (1 - \alpha)}{c_{\mathcal{G}} + \epsilon}. \end{aligned}$$

Combine with Eq. 12, finally,

$$\begin{aligned} & \Pr (T_r(\mathcal{F}, \mathcal{G}, x, y_t) = 1) \\ & \geq 1 - \eta_{\mathcal{F}} - \eta_{\mathcal{G}} - \alpha - \Pr (\mathcal{G}(x^A) \neq y_t) \\ & \stackrel{(i.)}{\geq} 1 - \eta_{\mathcal{F}} - \eta_{\mathcal{G}} - \alpha - \Pr \left(\delta \cdot \frac{\nabla_x \ell_{\mathcal{G}}(x, y_t)}{\|\nabla_x \ell_{\mathcal{G}}(x, y_t)\|_2} > g(x) \right) \\ & \geq 1 - \eta_{\mathcal{F}} - \eta_{\mathcal{G}} - \alpha - \frac{\epsilon(1 + \alpha) + \left(c_{\mathcal{F}} + \epsilon \sqrt{2 - 2 \underline{\mathcal{S}}(\ell_{\mathcal{F}}, \ell_{\mathcal{G}})} \right) (1 - \alpha)}{c_{\mathcal{G}} + \epsilon} \\ & = (1 - \alpha) - (\eta_{\mathcal{F}} + \eta_{\mathcal{G}}) - \frac{\epsilon(1 + \alpha) + c_{\mathcal{F}}(1 - \alpha)}{c_{\mathcal{G}} + \epsilon} - \frac{\epsilon(1 - \alpha)}{c_{\mathcal{G}} + \epsilon} \sqrt{2 - 2 \underline{\mathcal{S}}(\ell_{\mathcal{F}}, \ell_{\mathcal{G}})}. \end{aligned}$$

Here, (i.) follows Eq. 9. \square

Theorem (Lower Bound on Untargeted Attack Transferability). *Assume both models \mathcal{F} and \mathcal{G} are β -smooth. Let \mathcal{A}_U be an (α, \mathcal{F}) -effective untargeted attack with perturbation ball $\|\delta\|_2 \leq \epsilon$. The transferability can be lower bounded by*

$$\Pr(T_r(\mathcal{F}, \mathcal{G}, x) = 1) \geq (1-\alpha) - (\eta_{\mathcal{F}} + \eta_{\mathcal{G}}) - \frac{\epsilon(1+\alpha) - c_{\mathcal{F}}(1-\alpha)}{\epsilon - c_{\mathcal{G}}} - \frac{\epsilon(1-\alpha)}{\epsilon - c_{\mathcal{G}}} \sqrt{2 - 2\underline{\mathcal{S}}(\ell_{\mathcal{F}}, \ell_{\mathcal{G}})},$$

where

$$c_{\mathcal{F}} = \min_{(x,y) \in \text{supp}(\mathcal{D})} \frac{\min_{y' \in \mathcal{Y}: y' \neq y} \ell_{\mathcal{F}}(\mathcal{A}_U(x), y') - \ell_{\mathcal{F}}(x, y) - \beta\epsilon^2/2}{\|\nabla_x \ell_{\mathcal{F}}(x, y)\|_2},$$

$$c_{\mathcal{G}} = \max_{(x,y) \in \text{supp}(\mathcal{D})} \frac{\min_{y' \in \mathcal{Y}: y' \neq y} \ell_{\mathcal{G}}(\mathcal{A}_U(x), y') - \ell_{\mathcal{G}}(x, y) + \beta\epsilon^2/2}{\|\nabla_x \ell_{\mathcal{G}}(x, y)\|_2}.$$

Here $\eta_{\mathcal{F}}$ and $\eta_{\mathcal{G}}$ are the risks of models \mathcal{F} and \mathcal{G} respectively. The $\text{supp}(\mathcal{D})$ is the support of benign data distribution, i.e., x is the benign data and y is its associated true label.

Proof. For simplifying the notations, we define $x^{\mathcal{A}} := \mathcal{A}_U(x)$, which is the generated adversarial example by \mathcal{A}_U when the input is x . Define auxiliary function $f, g : \mathcal{M} \rightarrow \mathbb{R}$ such that

$$f(x, y) = \frac{\min_{y' \in \mathcal{Y}: y' \neq y} \ell_{\mathcal{F}}(x^{\mathcal{A}}, y') - \ell_{\mathcal{F}}(x, y) - \beta\epsilon^2/2}{\|\nabla_x \ell_{\mathcal{F}}(x, y)\|_2},$$

$$g(x, y) = \frac{\min_{y' \in \mathcal{Y}: y' \neq y} \ell_{\mathcal{G}}(x^{\mathcal{A}}, y') - \ell_{\mathcal{G}}(x, y) + \beta\epsilon^2/2}{\|\nabla_x \ell_{\mathcal{G}}(x, y)\|_2}.$$

The f and g are orthogonal to the confidence score functions of model \mathcal{F} and \mathcal{G} . Note that

$$c_{\mathcal{F}} = \min_{(x,y) \in \text{supp}(\mathcal{D})} f(x, y), c_{\mathcal{G}} = \max_{(x,y) \in \text{supp}(\mathcal{D})} g(x, y).$$

The proof is similar to that of Theorem 1.

$$\begin{aligned} & \Pr(T_r(\mathcal{F}, \mathcal{G}, x) = 1) \\ &= \Pr(\mathcal{F}(x) = y \cap \mathcal{G}(x) = y \cap \mathcal{F}(x^{\mathcal{A}}) \neq y \cap \mathcal{G}(x^{\mathcal{A}}) \neq y) \\ &\geq 1 - \Pr(\mathcal{F}(x) \neq y) - \Pr(\mathcal{G}(x) \neq y) - \Pr(\mathcal{F}(x^{\mathcal{A}}) = y) - \Pr(\mathcal{G}(x^{\mathcal{A}}) = y) \\ &= 1 - \eta_{\mathcal{F}} - \eta_{\mathcal{G}} - \alpha - \Pr(\mathcal{G}(x^{\mathcal{A}}) = y). \end{aligned} \quad (13)$$

From Taylor's Theorem and Lemma 7, we observe that

$$\Pr(\mathcal{G}(x^{\mathcal{A}}) = y) \leq \Pr\left(\delta \cdot \frac{\nabla_x \ell_{\mathcal{G}}(x, y)}{\|\nabla_x \ell_{\mathcal{G}}(x, y)\|_2} < c_{\mathcal{G}}\right), \quad (14)$$

$$\Pr\left(\delta \cdot \frac{\nabla_x \ell_{\mathcal{G}}(x, y)}{\|\nabla_x \ell_{\mathcal{G}}(x, y)\|_2} < c_{\mathcal{F}} - \epsilon\sqrt{2 - 2\underline{\mathcal{S}}(\ell_{\mathcal{F}}, \ell_{\mathcal{G}})}\right) \leq \Pr(\mathcal{F}(x^{\mathcal{A}}) = y) = \alpha. \quad (15)$$

According to Markov's inequality, Eq. 15 implies that

$$\Pr\left(\delta \cdot \frac{\nabla_x \ell_{\mathcal{G}}(x, y)}{\|\nabla_x \ell_{\mathcal{G}}(x, y)\|_2} < c_{\mathcal{G}}\right) \leq \frac{\epsilon(1+\alpha) - (c_{\mathcal{F}} - \epsilon\sqrt{2 - 2\underline{\mathcal{S}}(\ell_{\mathcal{F}}, \ell_{\mathcal{G}})})(1-\alpha)}{\epsilon - c_{\mathcal{G}}}. \quad (16)$$

We conclude the proof by combining Eq. 14 with Eq. 16 and plugging it into Eq. 13. \square

D Proof of Transferability Upper Bound (Theorems 2 and 4)

Here we present the proof of Theorem 2 and Theorem 4 as stated in Section 2.4 and Appendix A.

The following lemma is used in the proof.

Lemma 8. *Suppose two unit vectors x, y satisfy $x \cdot y \leq S$, then for any δ , we have $\min(\delta \cdot x, \delta \cdot y) \leq \|\delta\|_2 \sqrt{(1+S)/2}$.*

Proof. Denote α to be the angle between x and y , then $\cos \alpha \leq S$, or $\alpha \geq \arccos S$. If α_x, α_y are the angles between δ and x and between δ and y respectively, then we have $\max(\alpha_x, \alpha_y) \geq \alpha/2 \geq \arccos S/2$. By the half-angle formula, $\cos(\alpha/2) \leq \cos\left(\frac{\arccos S}{2}\right) = \sqrt{\frac{1+S}{2}}$. Thus, $\min(\delta \cdot x, \delta \cdot y) \leq \|\delta\|_2 \cos(\alpha/2) \leq \|\delta\|_2 \sqrt{(1+S)/2}$. \square

Theorem (Upper Bound on Targeted Attack Transferability). *Assume both model \mathcal{F} and \mathcal{G} are β -smooth with gradient magnitude bounded by B , i.e., $\|\nabla_x \ell_{\mathcal{F}}(x, y)\| \leq B$ and $\|\nabla_x \ell_{\mathcal{G}}(x, y)\| \leq B$ for any $x \in \mathcal{X}, y \in \mathcal{Y}$. Let \mathcal{A}_T be an (α, \mathcal{F}) -effective targeted attack with perturbation ball $\|\delta\|_2 \leq \epsilon$ and target label $y_t \in \mathcal{Y}$. When the attack radius ϵ is small such that $\ell_{\min} - \epsilon B \left(1 + \sqrt{\frac{1+\bar{\mathcal{S}}(\ell_{\mathcal{F}}, \ell_{\mathcal{G}})}{2}}\right) - \beta \epsilon^2 > 0$, the transferability can be upper bounded by*

$$\Pr(T_r(\mathcal{F}, \mathcal{G}, x, y_t) = 1) \leq \frac{\xi_{\mathcal{F}} + \xi_{\mathcal{G}}}{\ell_{\min} - \epsilon B \left(1 + \sqrt{\frac{1+\bar{\mathcal{S}}(\ell_{\mathcal{F}}, \ell_{\mathcal{G}})}{2}}\right) - \beta \epsilon^2},$$

where $\ell_{\min} = \min_{x \in \mathcal{X}} (\ell_{\mathcal{F}}(x, y_t), \ell_{\mathcal{G}}(x, y_t))$. Here $\xi_{\mathcal{F}}$ and $\xi_{\mathcal{G}}$ are the empirical risks of models \mathcal{F} and \mathcal{G} respectively, defined relative to a differentiable loss.

Proof. We let $x^A := \mathcal{A}_T(x)$ be the generated adversarial example when the input is x . Since $\mathcal{F}(x)$ outputs label for which $\ell_{\mathcal{F}}$ is minimized, we have

$$\mathcal{F}(x) = y \implies \ell_{\mathcal{F}}(x, y_t) > \ell_{\mathcal{F}}(x, y) \quad (17)$$

and similarly

$$\mathcal{F}(x^A) = y_t \implies \ell_{\mathcal{F}}(x^A, y) > \ell_{\mathcal{F}}(x^A, y_t), \quad (18)$$

$$\mathcal{G}(x) = y \implies \ell_{\mathcal{G}}(x, y_t) > \ell_{\mathcal{G}}(x, y), \quad (19)$$

$$\mathcal{G}(x^A) = y_t \implies \ell_{\mathcal{G}}(x^A, y) > \ell_{\mathcal{G}}(x^A, y_t). \quad (20)$$

Since $\ell_{\mathcal{F}}(x, y)$ and $\ell_{\mathcal{G}}(x, y)$ are β -smooth,

$$\ell_{\mathcal{F}}(x, y) + \delta \cdot \nabla_x \ell_{\mathcal{F}}(x, y) + \frac{\beta}{2} \|\delta\|^2 \geq \ell_{\mathcal{F}}(x^A, y),$$

which implies

$$\begin{aligned} \delta \cdot \nabla_x \ell_{\mathcal{F}}(x, y) &\geq \ell_{\mathcal{F}}(x^A, y) - \ell_{\mathcal{F}}(x, y) - \frac{\beta}{2} \|\delta\|^2 \\ &\geq \ell_{\mathcal{F}}(x^A, y_t) - \ell_{\mathcal{F}}(x, y) - \frac{\beta}{2} \|\delta\|^2 =: c'_{\mathcal{F}}. \end{aligned} \quad (21)$$

Similarly for \mathcal{G} ,

$$\delta \cdot \nabla_x \ell_{\mathcal{G}}(x, y) \geq \ell_{\mathcal{G}}(x^A, y_t) - \ell_{\mathcal{G}}(x, y) - \frac{\beta}{2} \|\delta\|^2 =: c'_{\mathcal{G}}. \quad (22)$$

Thus,

$$\begin{aligned} &\Pr(\mathcal{F}(x) = y, \mathcal{G}(x) = y, \mathcal{F}(x^A) = y_t, \mathcal{G}(x^A) = y_t) \\ &\leq \Pr(\ell_{\mathcal{F}}(x, y_t) > \ell_{\mathcal{F}}(x, y), \ell_{\mathcal{F}}(x^A, y) > \ell_{\mathcal{F}}(x^A, y_t), \ell_{\mathcal{G}}(x, y_t) > \ell_{\mathcal{G}}(x, y), \ell_{\mathcal{G}}(x^A, y) > \ell_{\mathcal{G}}(x^A, y_t)) \end{aligned} \quad (23)$$

$$\leq \Pr(\delta \cdot \nabla_x \ell_{\mathcal{F}}(x, y) \geq c'_{\mathcal{F}}, \delta \cdot \nabla_x \ell_{\mathcal{G}}(x, y) \geq c'_{\mathcal{G}}) \quad (24)$$

$$\leq \Pr\left(\left(c'_{\mathcal{F}} \leq \epsilon \sqrt{(1 + \bar{\mathcal{S}}(\ell_{\mathcal{F}}, \ell_{\mathcal{G}}))/2} \|\nabla_x \ell_{\mathcal{F}}(x, y)\|_2\right) \cup \left(c'_{\mathcal{G}} \leq \epsilon \sqrt{(1 + \bar{\mathcal{S}}(\ell_{\mathcal{F}}, \ell_{\mathcal{G}}))/2} \|\nabla_x \ell_{\mathcal{G}}(x, y)\|_2\right)\right) \quad (25)$$

$$\leq \Pr\left(c'_{\mathcal{F}} \leq \epsilon \sqrt{(1 + \bar{\mathcal{S}}(\ell_{\mathcal{F}}, \ell_{\mathcal{G}}))/2} \|\nabla_x \ell_{\mathcal{F}}(x, y)\|_2\right) + \Pr\left(c'_{\mathcal{G}} \leq \epsilon \sqrt{(1 + \bar{\mathcal{S}}(\ell_{\mathcal{F}}, \ell_{\mathcal{G}}))/2} \|\nabla_x \ell_{\mathcal{G}}(x, y)\|_2\right), \quad (26)$$

where Eq. 23 comes from Eqs. 17 to 20, Eq. 24 comes from Eq. 21 and Eq. 22. The Eq. 25 is a result of Lemma 8: either

$$\delta \cdot \frac{\nabla_x \ell_{\mathcal{F}}(x, y)}{\|\nabla_x \ell_{\mathcal{F}}(x, y)\|_2} \leq \|\delta\|_2 \sqrt{(1 + \overline{\mathcal{S}}(\ell_{\mathcal{F}}, \ell_{\mathcal{G}}))/2}$$

or

$$\delta \cdot \frac{\nabla_x \ell_{\mathcal{G}}(x, y)}{\|\nabla_x \ell_{\mathcal{G}}(x, y)\|} \leq \|\delta\|_2 \sqrt{(1 + \overline{\mathcal{S}}(\ell_{\mathcal{F}}, \ell_{\mathcal{G}}))/2}.$$

We observe that by β -smoothness condition of the loss function,

$$\begin{aligned} c'_{\mathcal{F}} &= \ell_{\mathcal{F}}(x^{\mathcal{A}}, y_t) - \ell_{\mathcal{F}}(x, y) - \frac{\beta}{2} \|\delta\|_2^2 \\ &\geq \ell_{\mathcal{F}}(x, y_t) + \delta \cdot \nabla_x \ell_{\mathcal{F}}(x, y_t) - \frac{\beta}{2} \|\delta\|_2^2 - \ell_{\mathcal{F}}(x, y) - \frac{\beta}{2} \|\delta\|_2^2. \end{aligned}$$

Thus,

$$\begin{aligned} &\Pr \left(c'_{\mathcal{F}} \leq \epsilon \sqrt{(1 + \overline{\mathcal{S}}(\ell_{\mathcal{F}}, \ell_{\mathcal{G}}))/2} \|\nabla_x \ell_{\mathcal{F}}(x, y)\|_2 \right) \\ &\leq \Pr \left(\ell_{\mathcal{F}}(x, y_t) - \ell_{\mathcal{F}}(x, y) \leq \epsilon B (1 + \sqrt{(1 + \overline{\mathcal{S}}(\ell_{\mathcal{F}}, \ell_{\mathcal{G}}))/2}) + \beta \epsilon^2 \right) \\ &\leq \Pr \left(\ell_{\mathcal{F}}(x, y) \geq \ell_{\mathcal{F}}(x, y_t) - \epsilon B (1 + \sqrt{(1 + \overline{\mathcal{S}}(\ell_{\mathcal{F}}, \ell_{\mathcal{G}}))/2}) - \beta \epsilon^2 \right) \\ &\leq \frac{\xi_{\mathcal{F}}}{\min_{x \in \mathcal{X}} \ell_{\mathcal{F}}(x, y_t) - \epsilon B \left(1 + \sqrt{(1 + \overline{\mathcal{S}}(\ell_{\mathcal{F}}, \ell_{\mathcal{G}}))/2} \right) - \beta \epsilon^2}. \end{aligned} \quad (27)$$

Similarly for \mathcal{G} ,

$$\begin{aligned} &\Pr \left(c'_{\mathcal{G}} \leq \epsilon \sqrt{(1 + \overline{\mathcal{S}}(\ell_{\mathcal{F}}, \ell_{\mathcal{G}}))/2} \|\nabla_x \ell_{\mathcal{G}}(x, y)\|_2 \right) \\ &\leq \frac{\xi_{\mathcal{G}}}{\min_{x \in \mathcal{X}} \ell_{\mathcal{G}}(x, y_t) - \epsilon B \left(1 + \sqrt{(1 + \overline{\mathcal{S}}(\ell_{\mathcal{F}}, \ell_{\mathcal{G}}))/2} \right) - \beta \epsilon^2}. \end{aligned} \quad (28)$$

We conclude the proof by combining the above two equations into Eq. 26. \square

Theorem (Upper Bound on Untargeted Attack Transferability). *Assume both model \mathcal{F} and \mathcal{G} are β -smooth with gradient magnitude bounded by B , i.e., $\|\nabla_x \ell_{\mathcal{F}}(x, y)\| \leq B$ and $\|\nabla_x \ell_{\mathcal{G}}(x, y)\| \leq B$ for any $x \in \mathcal{X}, y \in \mathcal{Y}$. Let A_U be an (α, \mathcal{F}) -effective untargeted attack with perturbation ball $\|\delta\|_2 \leq \epsilon$. When the attack radius ϵ is small such that $\ell_{\min} - \epsilon B \left(1 + \sqrt{\frac{1 + \overline{\mathcal{S}}(\ell_{\mathcal{F}}, \ell_{\mathcal{G}})}{2}} \right) - \beta \epsilon^2 > 0$, the transferability can be upper bounded by*

$$\Pr (T_r(\mathcal{F}, \mathcal{G}, x) = 1) \leq \frac{\xi_{\mathcal{F}} + \xi_{\mathcal{G}}}{\ell_{\min} - \epsilon B \left(1 + \sqrt{\frac{1 + \overline{\mathcal{S}}(\ell_{\mathcal{F}}, \ell_{\mathcal{G}})}{2}} \right) - \beta \epsilon^2},$$

where $\ell_{\min} = \min_{\substack{x \in \mathcal{X}, y' \in \mathcal{Y}: \\ (x, y) \in \text{supp}(\mathcal{D}), y' \neq y}} (\ell_{\mathcal{F}}(x, y'), \ell_{\mathcal{G}}(x, y'))$. Here $\xi_{\mathcal{F}}$ and $\xi_{\mathcal{G}}$ are the empirical risks of models \mathcal{F} and \mathcal{G} respectively, defined relative to a differentiable loss. The $\text{supp}(\mathcal{D})$ is the support of benign data distribution, i.e., x is the benign data and y is its associated true label.

Proof. The proof follows the proof for the targeted attack case. Accordingly, Eq. 21 and Eq. 22 are modified to

$$\begin{aligned} \delta \cdot \nabla_x \ell_{\mathcal{F}}(x, y) &\geq \ell_{\mathcal{F}}(x^{\mathcal{A}}, y) - \ell_{\mathcal{F}}(x, y) - \frac{\beta}{2} \|\delta\|_2^2 \\ &\geq \ell_{\mathcal{F}}(x^{\mathcal{A}}, y_a) - \ell_{\mathcal{F}}(x, y) - \frac{\beta}{2} \|\delta\|_2^2 =: c'_{\mathcal{F}}. \end{aligned} \quad (29)$$

$$\delta \cdot \nabla_x \ell_{\mathcal{G}}(x, y) \geq \ell_{\mathcal{G}}(x^{\mathcal{A}}, y_b) - \ell_{\mathcal{G}}(x, y) - \frac{\beta}{2} \|\delta\|_2^2 =: c'_{\mathcal{G}} \quad (30)$$

where y_a and y_b are the predicted labels of model \mathcal{F} and \mathcal{G} for x^A under a transferable untargeted attack respectively. Both y_a and y_b are not equal to y . Then, instead of $\min_{x \in \mathcal{X}} \ell_{\mathcal{F}/\mathcal{G}}(x, y_t)$ we use

$$\min_{x \in \mathcal{X}, y' \in \mathcal{Y}: (x, y) \in \text{supp}(\mathcal{D}), y' \neq y} \ell_{\mathcal{F}/\mathcal{G}}(x, y')$$

in Eq. 27 and Eq. 28 and henceforth. \square

E Additional Details for Baseline Ensembles and Whitebox Attacks

In this section, we present a detailed introduction for our baseline ensembles and evaluated whitebox attacks. We introduce the baseline ensemble methods as follows:

- **Boosting** [35, 43] is a natural way of model ensemble training, which builds different weak learners in a sequential manner improving diversity in handling different task partitions. Here we consider two variants of boosting algorithms: 1) **AdaBoost** [19], where the final prediction will be the weighted average of all the weak learners: weight α_i for i -th base model is decided by the accumulated error e_i as $\alpha_i = \log \frac{1-e_i}{e_i} + \log(K-1)$. Here K refers to the number of categories in a classification task. As we can see, higher weight will be placed on stronger learners. 2) **GradientBoost** [16], which is a general ensemble training method by identifying weaker learners based on gradient information and generating the ensemble by training base models step by step with diverse learning orientations within pseudo-residuals $r = -\frac{\partial \ell(f(x), y)}{\partial f(x)}$ computed from the current ensemble model f on input x with ground truth label y .
- **CKAE** [25] develops diverse ensembles based on CKA measurement, which is recently shown to be effective to measure the orthogonality between representations. For two representations K and L , $\text{CKA}(K, L) = \frac{\text{HSIC}(K, L)}{\sqrt{\text{HSIC}(K, K)\text{HSIC}(L, L)}}$, $\text{HSIC}(K, L) = \frac{1}{(n-1)^2} \text{tr}(KHLH)$, where n is the number of samples and H the centering matrix. For an ensemble consisting of base models $\{\mathcal{F}_i\}$, we regard the representation of \mathcal{F}_i as its loss gradient vectors on batch samples and then minimize pair-wise CKA between base models $\mathcal{F}_i, \mathcal{F}_j$'s representations to encourage ensemble diversity.
- **ADP** [38] is proposed recently as an effective regularization-based training method to reduce adversarial transferability among base models within an ensemble by maximizing the volume spanned by base models' non-maximal output vectors. Specifically, for a ensemble consisting of base models $\{\mathcal{F}_i\}_{i=1}^N$ and input x with ground truth label y , the ADP regularizer is defined as $\mathcal{L}_{\text{ADP}}(x, y) = \alpha \cdot H(\text{mean}(\{\mathcal{F}_i(x)\}_{i=1}^N)) + \beta \cdot \log(\mathbb{E}\mathbb{D})$, where $H(\cdot)$ is the Shannon Entropy Loss and $\mathbb{E}\mathbb{D}$ the square of the spanned volume. Nevertheless, the ADP ensemble has been shown to be vulnerable against attacks that run for enough iterations until converged [49]. We will also discuss this similar observation in our empirical robustness evaluation.
- **GAL** [23] promotes the diverse properties of the ensemble model by only minimizing the actual cosine similarities between pair-wise base models' loss gradient vectors. For N base models $\{\mathcal{F}_i\}_{i=1}^N$ within an ensemble and input x with ground truth label y , the GAL regularizer is defined as: $\mathcal{L}_{\text{GAL}} = \log(\sum_{1 \leq i < j \leq N} \exp(\text{CS}(\nabla_x \ell_{\mathcal{F}_i}, \nabla_x \ell_{\mathcal{F}_j}))$ where $\text{CS}(\cdot, \cdot)$ refers to the actual cosine similarity measurement and $\nabla_x \ell_{\mathcal{F}_i}$ the loss gradient of base model \mathcal{F}_i on x . It could serve as a baseline to empirically verify our theoretical analysis: when the loss gradients of base models are similar, the smoother the base models are, the less transferable they are.
- **DVERGE** [56] reduces the transferability among base models by utilizing Cross-Adversarial-Training: For a ensemble consisting of base models $\{\mathcal{F}_i\}$ and input x with ground truth label y , each base model \mathcal{F}_i is trained with the non-robust feature instances [22] generated against another base model. Specifically, DVERGE minimizes $\sum_{j \neq i} \ell(\mathcal{F}_i(x'_{\mathcal{F}_j}(x_s, x)), y_s)$ for every \mathcal{F}_i iteratively, where $x'_{\mathcal{F}_j}(x_s, x)$ represents the non-robust features against \mathcal{F}_j based on the randomly chosen input (x_s, y_s) . $\ell(\cdot, \cdot)$ is the cross-entropy loss function.

We consider the following attacks for whitebox robustness evaluation. Here we define (x, y) to be the input x with label y and x^A to be the notion of adversarial example generated from x . $\ell(\mathcal{F}(x), y)$ refers to the loss between model output $\mathcal{F}(x)$ and label y , and ϵ is the ℓ_∞ perturbation magnitude bound for different attacks.

- *Fast Gradient Sign Method* (FGSM) [17] is a simple yet effective attack strategy which generates adversarial example $x^A = x + \nu$ by assigning $\nu = \epsilon \cdot \text{sgn}(\nabla_x \ell(\mathcal{F}(x), y))$.

- *Basic Iterative Method* (BIM) [34] is an iterative attack method which adds adversarial perturbations step by step: $x_{i+1} = \text{clip}(x_i + \alpha \cdot \nabla_{x_i} \ell(\mathcal{F}(x_i), y))$, with initial starting point $x_0 = x$. Function $\text{clip}(\cdot)$ projects the perturbed instance back to the ℓ_∞ ball within the perturbation range ϵ , and α refers to the step size.
- *Momentum Iterative Method* (MIM) [13] can be regarded as the variant of BIM by utilizing the gradient momentum during the iterative attack procedure. Within iteration $i + 1$, we update new gradient as $g_{i+1} = \mu g_i + \frac{\ell(\mathcal{F}(x_i), y)}{\|\nabla_{x_i} \ell(\mathcal{F}(x_i), y)\|_1}$ and set $x_{i+1} = \text{clip}(x_i + \alpha \cdot g_{i+1})$ while μ refers to the momentum coefficient and α the step size.
- *Projected Gradient Descent* (PGD) [34] can be regarded as the variant of BIM by sampling x_0 randomly within the ℓ_p ball around x within radius ϵ . After initialization, it follows the standard BIM procedure by setting $x_{i+1} = \text{clip}(x_i + \alpha \cdot \nabla_{x_i} \ell(\mathcal{F}(x_i), y))$ on i -th attack iteration.
- *Auto-PGD* (APGD) [11] is a step-size free variant of PGD by configuring the step-size according to the overall iteration budgets and the progress of the current attack. Here we consider APGD-CE and APGD-DLR attack which use CrossEntropy (CE) and Difference of Logits Ratio (DLR) [11] loss as their loss function correspondingly.
- *Carlini & Wanger Attack* (CW) [5] accomplishes the attack by solving the optimization problem: $x^A := \min_{x'} \|x' - x\|_2^2 + c \cdot f(x', y)$, where c is a constant to balance the perturbation scale and attack success rate, and f is the adversarial attack loss designed to satisfy the sufficient and necessary condition of different attacks. For instance, the untargeted attack loss is represented as $f(x', y) = \max(\mathcal{F}(x')_y - \mathcal{F}(x')_{i \neq y}, -\kappa)$ while κ is a confidence variable with value 0.1 as default.
- *Elastic-net Attack* (EAD) [8] follows the similar optimization of CW Attack while considering both ℓ_2 and ℓ_1 distortion: $x^A := \min_{x'} \|x' - x\|_2^2 + \beta \|x' - x\|_1 + c \cdot f(x', y)$. Here β, c refer to the balancing parameters and $f(x', y) = \max(\mathcal{F}(x')_y - \mathcal{F}(x')_{i \neq y}, -\kappa)$ under untargeted attack setting. We set $\beta = 0.01, \kappa = 0.1$ as default.

In our experiments, we set 50 attack iterations with step size $\alpha = \epsilon/5$ for BIM, MIM attack and PGD attack with 5 random starts. For CW and EAD attacks, we set the number of attack iterations as 1000 and evaluate them with different constant c for different datasets.

F Training Details

We adapt ResNet-20 [20] as the base model architecture and Adam optimizer [24] in all of our experiments.

TRS training algorithm. We show the one-epoch TRS training algorithm pseudo code in Algorithm 1. We apply the mini-batch training strategy and train the TRS ensemble for M epochs ($M = 120$ for MNIST and $M = 200$ for CIFAR-10) in our experiments. To decide the δ within the local min-max procedure, we use the **Warm-up** strategy by linearly increasing the local ℓ_∞ ball’s radius δ from small initial δ_0 to the final δ_M along with the increasing of training epochs.

Baseline training details. For ADP and GAL, we follow the exact training configuration mentioned in their paper in both MNIST and CIFAR-10 experiments. For DVERGE, we set the same feature distillation $\epsilon = 0.07$ with step size as 0.007 for CIFAR-10 as they mentioned in their paper but set $\epsilon = 0.5$ with step size as 0.05 for MNIST since they did not conduct any MNIST experiments in their paper. We set training epochs as 120 for MNIST and 200 for CIFAR-10 and CIFAR-100 in baseline training.

TRS training details. For MNIST, we set the initial learning rate $\alpha = 0.001$ and train our TRS ensemble for 120 epochs by decaying the learning rate by 0.1 at 40-th and 80-th epochs. For CIFAR-10 and CIFAR-100 we set the initial learning rate $\alpha = 0.001$ and train our TRS ensemble for 200 epochs by decaying the learning rate by 0.1 at 100-th and 150-th epochs. For PGD Optimization within $\mathcal{L}_{\text{smooth}}$ approximation, we set step size $\tilde{\alpha} = \delta/3$ and the total number of steps T as 6 for both MNIST and CIFAR-10 experiments. We also leverage the ablation study about the convergence of PGD optimization w.r.t the robustness of TRS ensemble by varying $\tilde{\alpha}$ and T in I.5.

By configuring the default TRS ensemble training setting, we evaluated the average epoch training time for TRS and compared it to other baselines (ADP, GAL, DVERGE) on RTX 2080 single GPU device. Results are shown in Table 2.

Algorithm 1 TRS training framework in epoch m for an ensemble with N base models $\{\mathcal{F}_i\}$, with the total number of training epochs M .

```

1:  $\delta_m \leftarrow \delta_0 + (\delta_M - \delta_0) \cdot m/M$ 
2: for  $b = 1, \dots, B$  do
3:    $(x, y) \leftarrow$  training instances from  $b$ -th mini-batch
4:    $\mathcal{L}_{\text{Reg}} \leftarrow 0$ 
5:    $\mathcal{L}_{\text{ECE}} \leftarrow 0$ 
6:   for  $i = 1, \dots, N$  do
7:     for  $j = i + 1, \dots, N$  do
8:        $\mathcal{L}_{\text{Reg}} \leftarrow \mathcal{L}_{\text{Reg}} + \mathcal{L}_{\text{TRS}}(\mathcal{F}_i, \mathcal{F}_j, x, \delta_m)$ 
9:     end for
10:  end for
11:  for  $i = 1, \dots, N$  do
12:     $\mathcal{L}_{\text{ECE}} \leftarrow \mathcal{L}_{\text{ECE}} + \mathcal{L}_{\text{CE}}(\mathcal{F}_i(x), y)$ 
13:  end for
14:   $\mathcal{L}_{\text{Reg}} \leftarrow \mathcal{L}_{\text{Reg}} / \binom{N}{2}$ 
15:   $\mathcal{L}_{\text{ECE}} \leftarrow \mathcal{L}_{\text{ECE}} / N$ 
16:  for  $i = 1, \dots, N$  do
17:     $\nabla_{\mathcal{F}_i} \leftarrow \nabla_{\mathcal{F}_i}[\mathcal{L}_{\text{ECE}} + \mathcal{L}_{\text{Reg}}]$ 
18:     $\mathcal{F}_i \leftarrow \mathcal{F}_i - lr \cdot \nabla_{\mathcal{F}_i}$ 
19:  end for
20: end for

```

Table 2: Comparison on average epoch training time (s) between TRS training and other baseline training methods, evaluated on RTX 2080 single GPU device.

Avg epoch training time (s)	ADP	GAL	DVERGE	TRS
MNIST	29.22	106.81	184.42	302.24
CIFAR-10	33.22	139.10	349.61	1291.55

Our results show that though ADP, GAL require less training time, they can not achieve even comparable robustness with TRS as shown in our paper. Compared with DVERGE, TRS requires longer training time but maintains higher robustness under almost all attack scenarios.

G Numerical Results of Blackbox Robustness Evaluation

Table 3 and 4 show the detailed robust accuracy number of different ensembles against blackbox transfer attack with different perturbation scale ϵ , which corresponds to the Figure 2. As we can see, TRS ensemble shows its competitive robustness to DVERGE on small ϵ setting but much better stability of robustness on large ϵ setting although it slightly sacrifices benign accuracy on clean data.

H Statistical Stability Analysis on Robust Accuracy

For attacks with random-start (PGD, APGD-DLR, APGD-CE) mentioned in Table 1, we run each of them 10 times with different random seeds and evaluate them on TRS ensemble to present the statistical indicators (Min, Max, Mean, Std) of robust accuracy in Table 6. We can conclude that our reported robust accuracy shows statistical stability given the standard deviation is smaller than 0.3 under all the scenarios.

I Ablation Studies

I.1 Decision Boundary Analysis

We visualize the decision boundary of the GAL, DVERGE and TRS ensembles for MNIST and CIFAR-10 in Figure 4. The dashed line is the negative gradient direction and the horizontal direction

Table 3: Robust accuracy (%) of different approaches against **blackbox transfer attack** with different perturbation scales ϵ on MNIST dataset.

ϵ	clean	0.10	0.15	0.20	0.25	0.30	0.35	0.40
Vanilla	99.5	1.8	0.1	0.0	0.0	0.0	0.0	0.0
ADP	99.4	25.5	13.8	7.0	2.1	0.3	0.1	0.0
GAL	98.7	96.8	77.0	29.1	12.8	4.6	1.9	0.6
DVERGE	98.7	97.6	97.4	96.9	96.2	94.2	78.3	20.2
TRS	98.6	97.2	96.7	96.5	96.3	95.5	93.1	86.4

Table 4: Robust accuracy (%) of different approaches against **blackbox transfer attack** with different perturbation scales ϵ on CIFAR-10 dataset.

ϵ	clean	0.01	0.02	0.03	0.04	0.05	0.06	0.07
Vanilla	94.1	10.0	0.1	0.0	0.0	0.0	0.0	0.0
ADP	91.6	20.7	0.5	0.0	0.0	0.0	0.0	0.0
GAL	88.3	74.6	58.9	39.1	22.0	11.3	5.2	2.1
DVERGE	91.9	83.3	69.0	49.8	28.2	14.4	4.0	0.8
TRS	86.7	82.3	76.1	65.8	55.0	45.5	35.8	26.7

Table 5: Robust accuracy (%) of TRS ensemble trained with different hyper-parameter settings against various whitebox attacks on MNIST dataset.

λ_a		100				500			
λ_b		2.5		10		2.5		10	
δ_M		0.3	0.4	0.3	0.4	0.3	0.4	0.3	0.4
FGSM	$\epsilon = 0.1$	95.6	94.6	90.6	94.8	95.6	93.0	95.2	93.6
	$\epsilon = 0.2$	91.7	83.4	89.7	87.3	92.0	84.0	88.0	85.0
BIM (50)	$\epsilon = 0.1$	93.3	82.9	75.7	92.5	88.2	83.9	92.6	90.9
	$\epsilon = 0.15$	85.7	69.7	61.3	84.1	73.1	61.3	82.2	83.3
PGD (50)	$\epsilon = 0.1$	93.0	79.1	74.3	92.2	86.3	83.3	91.7	90.6
	$\epsilon = 0.15$	85.1	62.6	57.4	82.6	69.9	58.2	80.0	82.9
MIM (50)	$\epsilon = 0.1$	92.9	81.6	75.1	92.0	87.7	83.5	91.7	91.2
	$\epsilon = 0.15$	85.1	68.2	60.2	83.7	74.0	62.4	82.4	83.4
CW	$c = 0.1$	98.1	96.6	96.4	97.5	98.4	97.2	98.1	97.8
	$c = 1.0$	92.6	92.6	89.1	95.9	86.1	77.4	88.2	95.1
EAD	$c = 1.0$	23.3	14.3	9.2	24.1	22.5	2.6	3.4	23.9
	$c = 5.0$	1.4	0.9	0.1	2.3	0.0	0.0	0.2	1.7
APGD-DLR	$\epsilon = 0.1$	92.1	78.5	72.8	91.5	85.9	82.8	91.1	90.2
	$\epsilon = 0.15$	83.4	62.1	57.0	82.3	69.6	57.9	79.8	82.4
APGD-CE	$\epsilon = 0.1$	91.7	78.1	72.1	91.2	85.2	82.5	90.8	89.7
	$\epsilon = 0.15$	82.8	61.3	56.5	81.9	69.3	57.6	79.4	81.7

Table 6: {Min, Max, Mean, Std} of Robust accuracy (%) of TRS ensemble against 10 times whitebox attacks simulation with different random seeds on MNIST and CIFAR-10 datasets.

Robust Accuracy		param.	Min	Max	Mean	Std
MNIST	PGD	$\epsilon = 0.1$	92.8	93.2	93.1	0.143
		$\epsilon = 0.15$	84.9	85.1	85.1	0.067
	APGD-DLR	$\epsilon = 0.1$	92.1	92.3	92.2	0.083
		$\epsilon = 0.15$	83.2	83.5	83.4	0.114
	APGD-CE	$\epsilon = 0.1$	91.7	92.0	91.9	0.102
		$\epsilon = 0.15$	82.5	82.9	82.7	0.120
CIFAR-10	PGD	$\epsilon = 0.01$	50.4	50.5	50.4	0.049
		$\epsilon = 0.02$	14.8	15.8	15.2	0.293
	APGD-DLR	$\epsilon = 0.01$	50.0	50.5	50.2	0.151
		$\epsilon = 0.02$	15.2	16.0	15.6	0.234
	APGD-CE	$\epsilon = 0.01$	48.6	48.9	48.8	0.090
		$\epsilon = 0.02$	15.3	16.0	15.6	0.199

is randomly chosen which is orthogonal to the gradient direction. From the decision boundary of GAL ensemble, we can see that controlling only the gradient similarity will lead to a very non-smooth

Table 7: Conditional Robust Accuracy (%) of Adversarial Training based ensemble (AdvT) and TRS+AdvT ensemble against (Top) **whitebox attacks** and (Down) **blackbox attack** with different perturbation scales ϵ .

Attacks		FGSM		BIM (50)		PGD (50)		MIM (50)	
MNIST	ϵ	0.10	0.20	0.10	0.15	0.10	0.15	0.10	0.15
	AdvT	98.4	97.3	98.2	97.5	98.2	97.2	98.2	97.6
	TRS+AdvT	99.1	98.0	99.0	98.2	98.9	98.0	99.0	98.1
CIFAR-10	ϵ	0.02	0.04	0.01	0.02	0.01	0.02	0.01	0.02
	AdvT	79.3	60.0	88.5	76.1	88.4	76.1	88.5	76.3
	TRS+AdvT	79.2	58.0	90.7	76.7	90.7	76.6	90.9	76.9

MNIST	ϵ	0.10	0.15	0.20	0.25	0.30	0.35	0.40
	AdvT	98.9	98.7	98.6	98.4	98.4	91.6	8.1
	TRS+AdvT	99.4	99.3	99.1	99.1	98.9	98.7	98.5
CIFAR-10	ϵ	0.01	0.02	0.03	0.04	0.05	0.06	0.07
	AdvT	98.4	96.2	93.9	91.5	89.0	84.9	81.1
	TRS+AdvT	98.8	97.7	94.9	92.6	89.9	86.3	81.6

model decision boundary and thus harm the model robustness. From the comparison of DVERGE and TRS ensemble, we find that DVERGE ensemble tends to be more robust along the gradient direction especially on CIFAR-10, (i.e. the distance to the boundary is larger and sometimes even larger than along the other random direction). This may be due to the reason that DVERGE is essentially performing adversarial training for different base models and therefore it protects the adversarial (gradient) direction. Thus, DVERGE performs better against weak attacks which only consider the gradient direction (e.g. FGSM on CIFAR-10). On the other hand, we find that TRS training yields a smoother model along different directions than DVERGE, which leads to more consistent predictions within a large neighborhood of an input. Thus, the TRS ensemble has higher robustness in different directions against strong attacks such as PGD attack.

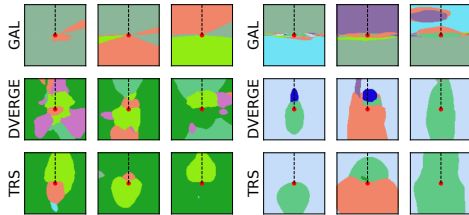


Figure 4: The decision boundary of different models around testing images on (left) MNIST and (right) CIFAR-10 dataset. Same color indicates the same model prediction. The dash lines shows the negative gradient direction, which is used in the gradient-based attacks.

I.2 TRS with Adversarial Training

While the TRS regularizer could reduce adversarial transferability among base models by enforcing low similarity on loss gradients and promoting model smoothness, we explore whether Adversarial Training [34], which aims to reduce base models' vulnerability, is able to further improve the robustness of TRS or not. We first apply adversarial training to train an ensemble model (AdvT) containing 3 base models as in TRS ensemble. During training, we use ℓ_∞ adversarial perturbation δ_{adv} ($\|\delta_{adv}\|_\infty \leq 0.2$ for MNIST and $\|\delta_{adv}\|_\infty \leq 0.03$ for CIFAR-10). To combine TRS with adversarial training (TRS+AdvT), we combine TRS regularizer Loss \mathcal{L}_{TRS} with Adversarial Training Loss $\mathcal{L}_{AdvT} = \max_{\|x-x'\|_\infty \leq \delta_{adv}} \ell_{\mathcal{F}}(x', y)$ on input x with label y with the same weight, and train the ensemble \mathcal{F} jointly. We evaluate both whitebox and blackbox robustness of TRS+AdvT and AdvT ensembles. During the evaluation, we consider the *Conditional Robust Accuracy* evaluated on adversarial examples generated based on correctly classified clean samples to eliminate the influence of model benign accuracy. Other settings are the same as we have introduced in Section 4.1.

Table 7 shows the robustness of both AdvT and TRS+AdvT under whitebox and blackbox attacks on different datasets. As we can see, TRS+AdvT ensemble outperforms the traditional adversarial training based ensemble consistently especially when ϵ is large.

I.3 Impacts of \mathcal{L}_{sim} and $\mathcal{L}_{\text{smooth}}$

To better understand the exact effects of regularizing \mathcal{L}_{sim} and $\mathcal{L}_{\text{smooth}}$, we conduct ablation studies by regularizing \mathcal{L}_{sim} or $\mathcal{L}_{\text{smooth}}$ only on both MNIST and CIFAR-10 datasets. Results are shown in Table 8.

We can see that, though training with $\mathcal{L}_{\text{smooth}}$ only could lead to high robustness, TRS ensemble could achieve even higher robustness against strong multi-step attacks by concerning similarity loss \mathcal{L}_{sim} at the same time. This indicates that both model smoothness and model diversity are important, though $\mathcal{L}_{\text{smooth}}$ would take the majority.

Table 8: Robust accuracy (%) of TRS ensemble trained by regularizing \mathcal{L}_{sim} or $\mathcal{L}_{\text{smooth}}$ only, or together, against various white-box attacks on MNIST and CIFAR-10 datasets.

Robust Accuracy		FGSM	BIM	PGD	MIM	CW	EAD
MNIST	param.	$\epsilon = 0.2$	$\epsilon = 0.15$	$\epsilon = 0.15$	$\epsilon = 0.15$	$c = 1.0$	$c = 10.0$
	\mathcal{L}_{sim} only	30.7	0.0	0.0	0.0	58.6	0.5
	$\mathcal{L}_{\text{smooth}}$ only	93.1	82.5	80.7	82.6	86.2	1.2
	$\mathcal{L}_{\text{sim}} + \mathcal{L}_{\text{smooth}}$ (TRS)	91.7	85.7	85.1	85.1	92.6	1.4
CIFAR-10	param.	$\epsilon = 0.04$	$\epsilon = 0.02$	$\epsilon = 0.02$	$\epsilon = 0.02$	$c = 1.0$	$c = 5.0$
	\mathcal{L}_{sim} only	35.0	0.0	0.0	0.0	17.6	0.0
	$\mathcal{L}_{\text{smooth}}$ only	9.3	13.9	13.8	15.0	43.0	0.0
	$\mathcal{L}_{\text{sim}} + \mathcal{L}_{\text{smooth}}$ (TRS)	24.9	15.8	15.1	17.2	58.1	0.1

I.4 Robust Accuracy Convergence Analysis

We observe that when the number of attack iterations is large, both ADP and GAL regularizer trained ensembles achieve much lower robust accuracy against iterative attacks (BIM, PGD, MIM) than the reported robustness in the original papers which is estimated under a small number of attack iterations. This case implies the non-convergence of iterative attack evaluation mentioned in their papers, which is also confirmed by [49]. In contrast, both DVERGE and TRS still remain highly robust against iterative attacks with large iterations. To show the stability of our model’s robust accuracy, we evaluate it against PGD attack with 500 and 1000 attack iterations. Results are shown in Table 9 where TRS ensemble’s robust accuracy only slightly drops after increasing the attack iterations, and outperforms DVERGE by a large margin.

I.5 Convergence of PGD Optimization within $\mathcal{L}_{\text{smooth}}$ Approximation

Since the computation cost of training a TRS ensemble partially relies on the complexity of PGD procedure on solving the inner-maximization task of $\mathcal{L}_{\text{smooth}}$, we conduct ablation study on analyzing the trade-off between the computation cost (by varying PGD steps T) and the resulting robustness of TRS ensemble on MNIST dataset. Specifically, we consider the following settings of PGD step size $\tilde{\alpha}$ and the number of steps T :

- (1) $\tilde{\alpha} = \delta, T = 1$
- (2) $\tilde{\alpha} = \delta/3, T = 6$
- (3) $\tilde{\alpha} = \delta/10, T = 20$

Results are shown in Table 10. As we can see, the robustness of TRS ensemble consistently improves with the increasing of T and converges. We should also notice that, even for $T = 1$, TRS ensemble is more robust than the strongest baseline DVERGE against various strong attacks. Due to the positive correlation between T and the training cost, we should choose suitable T balancing the training cost and model robustness. For MNIST, the default setting ($T = 6$) could be a good choice.

J Robustness of TRS Ensemble against Other Strong Blackbox Attacks

We also conduct additional blackbox robustness evaluation against the following three strong blackbox attacks which focus on attack transferability between surrogate model and target model:

Table 9: Convergence of PGD attack on different ensembles.

Settings		iters	ADP	GAL	DVERGE	TRS
MNIST	$\epsilon = 0.10$	50	4.5	4.1	69.2	93.0
		500	1.6	1.1	66.5	92.8
		1000	1.6	1.0	66.3	92.6
	$\epsilon = 0.15$	50	1.0	0.6	28.8	85.1
		500	0.5	0.1	25.0	83.6
		1000	0.4	0.1	24.8	83.5
CIFAR-10	$\epsilon = 0.01$	50	9.0	8.3	37.1	50.5
		500	3.5	7.8	35.8	50.3
		1000	2.9	7.8	35.7	50.2
	$\epsilon = 0.02$	50	0.1	0.6	10.5	15.1
		500	0.0	0.3	9.0	14.5
		1000	0.0	0.3	8.8	14.5

Table 10: Robustness of TRS ensemble against various white-box attacks by varying PGD step size $\tilde{\alpha}$ and total number of steps T for solving the inner-maximization within $\mathcal{L}_{\text{smooth}}$ on MNIST dataset.

Robust acc on MNIST	FGSM	BIM	PGD	MIM	CW	EAD
param.	$\epsilon = 0.2$	$\epsilon = 0.15$	$\epsilon = 0.15$	$\epsilon = 0.15$	$c = 1.0$	$c = 10.0$
DVERGE	91.6	47.7	28.8	44.6	79.2	0.0
TRS ($\tilde{\alpha} = \delta, T = 1$)	90.5	76.0	70.1	73.3	89.6	0.1
TRS ($\tilde{\alpha} = \delta/3, T = 6$)	91.7	85.7	85.1	85.1	92.6	1.4
TRS ($\tilde{\alpha} = \delta/10, T = 20$)	92.1	87.2	85.5	86.1	92.8	1.4

Table 11: Robust accuracy (%) of different approaches against strong blackbox transfer attack on MNIST and CIFAR-10 datasets.

Robust Accuracy		ILA	DI2-FGSM	IRA
MNIST ($\epsilon = 0.3$)	ADP	5.4	9.9	4.8
	GAL	3.0	8.6	7.1
	DVERGE	89.5	91.6	82.0
	TRS	91.2	93.7	84.4
CIFAR-10 ($\epsilon = 0.05$)	ADP	1.2	1.6	1.4
	GAL	32.2	36.2	29.2
	DVERGE	35.9	38.3	32.4
	TRS	46.2	50.0	45.1

- *Intermediate Level Attack* (ILA) [21] enhances the blackbox attack transferability by taking the perturbation on an intermediate layer of surrogate model into account.
- *DI2-FGSM* [55] can be viewed as a variant of BIM by applying input transformation randomly at each attack iteration to promote diverse input patterns.
- *Interaction Reduced Attack* (IRA) [50] integrates an additional interaction loss term after analyzing the negative correlation between attack transferability and interaction between adversarial units.

We use the open-source code mentioned in their original papers and generate blackbox adversarial examples from a surrogate ensemble model consisting of three ResNet20 submodels for both MNIST and CIFAR-10 datasets. We compare the robustness of TRS ensemble with other baseline ensemble. Results are shown in Table 11.

We can find that, TRS ensemble consistently demonstrates the highest robustness compared to other baseline ensembles, which indicates solid blackbox robustness of TRS ensemble against various types of blackbox attacks.

K Robustness of TRS Ensemble on CIFAR-100 Dataset

Besides MNIST and CIFAR-10 datasets, we also evaluate our proposed TRS ensemble on the CIFAR-100 dataset. The base model structure and training parameter configuration remain the same as in CIFAR-10 experiments. The whitebox robustness evaluation results are shown in Table 12. From the results, we can see that the robustness of TRS model is better than other methods against all attacks except FGSM, which is similar with our observations in CIFAR-10. This shows that our TRS algorithm still achieves a good performance on classification tasks with large number of classes.

Table 12: Robust accuracy(%) of different ensembles against whitebox attacks on CIFAR-100. “para.” refers to the attack parameter (ϵ is the ℓ_∞ perturbation budget for the attack and c the constant to balance the attack stealthiness and effectiveness).

CIFAR-100	para.	ADP	GAL	DVERGE	TRS
FGSM	$\epsilon = 0.02$	11.5	28.7	29.7	19.3
	$\epsilon = 0.04$	6.4	2.7	25.4	9.5
BIM (50)	$\epsilon = 0.01$	0.5	7.6	12.1	22.9
	$\epsilon = 0.02$	0.0	1.5	2.9	5.4
PGD (50)	$\epsilon = 0.01$	0.4	5.4	11.3	23.0
	$\epsilon = 0.02$	0.0	1.1	2.0	5.3
MIM (50)	$\epsilon = 0.01$	0.5	5.7	13.1	23.4
	$\epsilon = 0.02$	0.0	0.5	2.6	6.2
CW	$c = 0.01$	11.3	32.0	44.8	45.7
	$c = 0.1$	0.5	10.7	20.3	26.9
EAD	$c = 1.0$	0.0	0.0	1.0	5.7
	$c = 5.0$	0.0	0.0	0.0	0.3
APGD-LR	$\epsilon = 0.01$	0.2	4.3	11.8	22.2
	$\epsilon = 0.02$	0.0	0.6	2.1	5.3
APGD-CE	$\epsilon = 0.01$	0.2	4.2	11.3	20.7
	$\epsilon = 0.02$	0.0	0.4	1.7	4.8